

University of Windsor

## Scholarship at UWindor

---

Electronic Theses and Dissertations

Theses, Dissertations, and Major Papers

---

12-14-2018

# Relativistic Corrections to Nonrelativistic Electric Dipole Transitions

Daniel Venn  
*University of Windsor*

Follow this and additional works at: <https://scholar.uwindsor.ca/etd>

---

### Recommended Citation

Venn, Daniel, "Relativistic Corrections to Nonrelativistic Electric Dipole Transitions" (2018). *Electronic Theses and Dissertations*. 7627.  
<https://scholar.uwindsor.ca/etd/7627>

This online database contains the full-text of PhD dissertations and Masters' theses of University of Windsor students from 1954 forward. These documents are made available for personal study and research purposes only, in accordance with the Canadian Copyright Act and the Creative Commons license—CC BY-NC-ND (Attribution, Non-Commercial, No Derivative Works). Under this license, works must always be attributed to the copyright holder (original author), cannot be used for any commercial purposes, and may not be altered. Any other use would require the permission of the copyright holder. Students may inquire about withdrawing their dissertation and/or thesis from this database. For additional inquiries, please contact the repository administrator via email ([scholarship@uwindsor.ca](mailto:scholarship@uwindsor.ca)) or by telephone at 519-253-3000ext. 3208.

# Relativistic Corrections to Nonrelativistic Electric Dipole Transitions

By

Daniel Venn

A Thesis

Submitted to the Faculty of Graduate Studies  
through the Department of Physics  
in Partial Fulfillment of the Requirements for  
the Degree of Master of Science  
at the University of Windsor

Windsor, Ontario, Canada

2018

©2018, Daniel Venn

# Relativistic Corrections to Nonrelativistic Electric Dipole Transitions

by

Daniel Venn

APPROVED BY:

---

J.W. Gault

Department of Chemistry and Biochemistry

---

E.H. Kim

Department of Physics

---

G.W.F. Drake, Advisor

Department of Physics

December 14, 2018

# Declaration of Originality

I hereby certify that I am the sole author of this thesis and that no part of this thesis has been published or submitted for publication.

I declare that, to the best of my knowledge, my thesis does not infringe upon anyones copyright nor violate any proprietary rights and that any ideas, techniques, quotations, or any other material from the work of other people included in my thesis, published or otherwise, are fully acknowledged in accordance with the standard referencing practices. Furthermore, to the extent that I have included copyrighted material that surpasses the bounds of fair dealing within the meaning of the Canada Copyright Act, I certify that I have obtained a written permission from the copyright owner(s) to include such material(s) in my thesis.

# Abstract

Radiative transition probabilities for light atoms and ions are normally calculated from nonrelativistic wave functions and the electric dipole transition operator. For the nonrelativistic energies, the theory of relativistic corrections is well established in terms of the Breit interaction, but the same is not true for relativistic corrections to transition probabilities. The main focus of this work is to perform high precision variational calculations for the relativistic corrections for the case of allowed electric dipole transitions, and to compare with known results for the one-electron case. The calculation involves the use of perturbation theory, using pseudostates to sum over the complete sets of intermediate states. In the limit of large  $Z$ , it is only the leading hydrogenic term in a  $1/Z$  expansion that contributes, and so a direct check with the one-electron case is made in the thesis in order to establish a direct connection with transition matrix elements calculated directly from the Dirac equation. Given their importance in these calculations, this work also provides a test of general perturbation techniques and the rate of convergence with basis set size for relativistic perturbation operators.

# Acknowledgements

First, I would like to thank Dr. Gordon Drake for the opportunity to pursue my Master's degree under his guidance, as well as his continued support over the years.

Second, I would like to thank the research group, whose company was indispensable and will be certainly sorely missed.

Third, I would like to thank my family, whose patience knows no bounds.

# Contents

Declaration of Originality	iii
Abstract	iv
Acknowledgements	v
List of Figures	viii
List of Tables	x
<b>1 Background</b>	<b>1</b>
<b>2 Introduction</b>	<b>7</b>
2.1 Dirac Relativistic Theory . . . . .	7
2.2 Applications to Many-Electron Atoms . . . . .	7
<b>3 Mathematical Models for Atomic Systems</b>	<b>10</b>
3.1 Nonrelativistic Hydrogen . . . . .	10
3.2 Nonrelativistic Helium . . . . .	14
3.2.1 Correlated Variational Basis Sets . . . . .	15
3.2.2 Evaluating Matrix Elements . . . . .	20
3.3 Relativistic Corrections . . . . .	22

<b>4</b>	<b>Calculations</b>	<b>25</b>
4.1	Pseudospectral Convergence . . . . .	26
4.2	Nuclear Charge Scaling . . . . .	39
4.3	Comparisons with Schrödinger Technique . . . . .	43
<b>5</b>	<b>Conclusion</b>	<b>46</b>
	<b>Appendix A The Breit Equation</b>	<b>48</b>
	<b>Appendix B Computational Details</b>	<b>53</b>
	<b>Bibliography</b>	<b>57</b>
	<b>Vita Auctoris</b>	<b>59</b>



# List of Figures

3.1	Hylleraas coordinate system for a helium atom with the nucleus at the origin. . . . .	14
3.2	Hylleraas-Undheim-Macdonald Theorem, also known as the interleaving theorem [1] . . . . .	19
4.1	Convergence of $p^4 1s2p \ ^1P$ state perturbation contribution with increasing basis set size. . . . .	29
4.2	Convergence of $\delta(r_1) 1s2p \ ^1P$ state perturbation contribution with increasing basis set size. . . . .	29
4.3	Convergence of $\delta(r_{12}) 1s2p \ ^1P$ state perturbation contribution with increasing basis set size. . . . .	30
4.4	Convergence of spin-orbit $1s2p \ ^1P$ state perturbation contribution with increasing basis set size. . . . .	30
4.5	Convergence of $p^4 1s^2 \ ^1S$ state perturbation contribution with increasing basis set size. . . . .	32
4.6	Convergence of $\delta(r_1) 1s^2 \ ^1S$ state perturbation contribution with increasing basis set size. . . . .	33
4.7	Convergence of $\delta(r_{12}) 1s^2 \ ^1S$ state perturbation contribution with increasing basis set size. . . . .	34
4.8	Comparative convergence of $1s^2 \ ^1S$ and $1s2p \ ^1P$ state perturbation contributions. . . . .	36

4.9	$Z$ expansion of the $p^4$ contribution from the initial state. . . . .	43
4.10	$Z^{-1}$ expansion, with inherent $Z$ -scaling factored out, to compare with hydrogenic values. . . . .	44

# List of Tables

3.1	Example of basis set for the case $\Omega = 0$ and 1 . . . . .	17
4.1	$\langle \psi_{1s}^{(1)}   z   \psi_{2p}^{(0)} \rangle$ , initial state relativistic contributions. . . . .	27
4.2	$\langle \psi_{1s}^{(0)}   z   \psi_{2p}^{(1)} \rangle$ , final state relativistic contributions. . . . .	28
4.3	$1s^2 \ ^1S$ state contributions to the relativistic corrections to the transition probability, for the case of helium. . . . .	38
4.4	$1s2p \ ^1P$ state contributions to the relativistic corrections to the transition probability, for the case of helium. . . . .	38
4.5	Nuclear charge $Z$ scaling of the initial state contributions. . . . .	40
4.6	Nuclear charge $Z$ scaling of the final state contributions. . . . .	41
4.7	Relativistic corrections to transition probability, in comparison with hydrogenic values. . . . .	45

# Chapter 1

## Background

The basic goal of this work is to expand upon the current state of high precision calculations for helium by studying higher-order relativistic corrections for transition probabilities. Although helium has two electrons, for the case of one-electron hydrogen exact analytic solutions to the Schrödinger equation already exist [1]. This makes hydrogen a useful starting point for establishing and testing the techniques to be applied to helium. Relativistic corrections to nonrelativistic energies are already well established using the Breit interaction, but the same cannot be said for relativistic corrections to transition probabilities. A traditional start to determining radiative transition probabilities begins with nonrelativistic wave functions and the electric dipole transition operator [2]. The overall strategy is to find equivalent nonrelativistic operators such that, when matrix elements are calculated in terms of solutions to the nonrelativistic Schrödinger equation, they yield the same results as obtained from matrix elements of relativistic operators evaluated in terms of solutions to the relativistic Dirac equation. Both approaches involve an expansion in terms of the fine structure constant  $\alpha \simeq 1/137$  in atomic units. The equivalence can be expressed

mathematically in the form

$$\begin{aligned} \langle \psi_{rel} | T_{rel} | \phi_{rel} \rangle = & \langle \psi_{nr}^{(0)} | T_{nr}^{(0)} | \phi_{nr}^{(0)} \rangle + \alpha^2 \langle \psi_{nr}^{(1)} | T_{nr}^{(0)} | \phi_{nr}^{(0)} \rangle \\ & + \alpha^2 \langle \psi_{nr}^{(0)} | T_{nr}^{(0)} | \phi_{nr}^{(1)} \rangle + \alpha^2 \langle \psi_{nr}^{(0)} | T_{nr}^{(1)} | \phi_{nr}^{(0)} \rangle + O(\alpha^4) \end{aligned} \quad (1.1)$$

where  $\psi_{rel}$  and  $\phi_{rel}$  are solutions to the relativistic Dirac equation, and  $\psi_{nr}$  and  $\phi_{nr}$  are solutions to the nonrelativistic Schrodinger equation. Given a relativistic operator  $T_{rel}$ , the problem is to find equivalent nonrelativistic operators  $T_{nr}^{(0)}$ ,  $T_{nr}^{(1)}$ , and relativistically corrected wave functions  $\psi_{nr}^{(1)}$  and  $\phi_{nr}^{(1)}$ . For example, the Dirac operator  $T_{rel} = \alpha$  can be replaced in lowest order by the nonrelativistic operator  $T_{nr}^{(0)} = \mathbf{p}/mc$ , where  $\mathbf{p}$  is the momentum operator. This work can be broadly categorized as atomic theory; a field which itself is divided into two main topics. The first is concerned with the energy levels of atoms and the resulting wavelengths of the light that is emitted. The second is concerned with the rates of processes via cross sections for collisions, and the Einstein A and B coefficients for radiation. This is the subsection to which this work will contribute.

One method for analytically observing parts of the universe that we are not close enough to probe directly is to analyze the radiation emitted from atoms and molecules in the remote source. In order to correctly interpret and decode this radiation information, one needs an understanding of the relevant atomic and molecular processes that occur in different astrophysical circumstances such as supernovas or solar fusion. Specifically, relativistic corrections are of order  $(Z\alpha)^2$  which implies that atoms with higher nuclear charge have more significant relativistic corrections. Highly ionized atoms are present in astronomical plasmas such as solar corona, where temperatures can be as high as millions of Kelvin, or in fusion reactors such as tokamak reactors. This makes relativistic corrections an important quantity to calculate, especially for the case of highly ionized atoms.

Underlying the spectra of astronomical sources of radiation are quantities such

as oscillator strengths, rate coefficients for radiative, dielectronic, and dissociative recombination, transition frequencies, hyperfine structure transitions, and so on. As an introduction to this topic, let us look at an example of the importance of oscillator strengths in the context of astronomy.

Luminosity is a measure of the energy emitted per unit time by an astronomical object. More specifically, the luminosity of a planet can be classified as dayglow, nightglow, or aurora. Dayglow refers to the section of the planet facing its sun, known as its dayside. This dayglow is a result of the atmospheric interaction with solar radiation from its sun, resulting in photodissociative excitation,



and simultaneous dissociation and excitation,



and ionization and excitation,



or resonance scattering [3]. The above equations refer to electron impact processes, which produce excited states that are related to the ground state by either dipole allowed or forbidden transitions, whereas the focus of this work is on dipole allowed transitions which correspond to resonance and fluorescent scattering. In resonance scattering, the absorption of a photon by an atom in the ground state excites it into a higher state



where it then decays back to the ground state,

$$A^* \rightarrow A + h\nu \quad (1.6)$$

emitting a photon which has a wavelength essentially identical to the absorbed photon.

The absorption cross section is

$$\sigma_{12}^a(\nu) = \frac{\bar{\omega}_2}{\bar{\omega}_1} \frac{c^2}{8\pi\nu^2} A_{21} \phi(\nu) \quad (1.7)$$

where 1 and 2 indicate the lower and upper state respectively,  $\bar{\omega}$  is the statistical weight of the state,  $\nu$  is the frequency of the transition, and  $\phi(\nu)$  is the lineshape function, which is normalized such that the integral over all frequencies is unity [3].

Integrating the absorption cross section  $\sigma_{12}^a$  over all frequencies yields

$$\int_0^\infty \sigma_{12}^a(\nu) d\nu = \frac{\pi e^2}{m_e c} f_{12} \quad (1.8)$$

where  $m_e$  is the mass of the electron. Given this, the relation between  $A_{21}$  and the oscillator strength is

$$A_{21} = \frac{\bar{\omega}_1}{\bar{\omega}_2} \frac{8\pi^2 e^2 \nu^2}{m_e c^3} f_{12} = \frac{\bar{\omega}_1}{\bar{\omega}_2} \frac{8\pi^2 e^2}{m_e c \lambda^2} f_{12} \quad (1.9)$$

where  $\lambda$  is the wavelength of the emitted photon [3]. From this we can get the excitation rate  $q_2$  due to resonance scattering, given by

$$q_2 = F(\nu) \frac{\pi e^2}{m_e c} f_{12} = F(\lambda) \frac{\bar{\omega}_2}{\bar{\omega}_1} \frac{\lambda^4}{8\pi c} A_{21} \quad (1.10)$$

where  $F(\nu)$  is the solar photon flux. There are two notes here regarding conventions in aeronomy; the first is that the solar flux  $F(\nu)$  is sometimes denoted as  $\pi F(\nu)$ , and the second is defining a “ $g$ -factor” as the probability per atom that a photon will be

resonantly scattered such that

$$g_{21} = q_2 A_{21} / \sum_i A_{2i} \quad (1.11)$$

where the sum in the denominator refers to all the states  $i$  below the upper state 2 [3]. The  $g$ -factor for unattenuated solar radiation is used at the average distance between the solar body and the planet in question, and its used to calculate the volume emission rate as well.

Although the scope of this work includes only atomic systems rather than molecular ones, it is worth noting that in fluorescent scattering, where a molecule in a vibrational state absorbs and then emits a photon, the properties of excitation and emission rate are calculated using the transition probability between the two states. The quantities calculated in this work, and the field of atomic theory generally, find their relevance in many different applications. The helium atom has a geometrically simple shape yet a mathematically complex form, and so its nucleus and two electrons secures it a fundamental and interesting position in the domain of atomic theory. The Schrödinger equation for helium is the first instance on the periodic table of elements that has a three-body system. This makes helium a useful system to experiment with, for other more general three-body systems. With the introduction of the Schrödinger equation in 1925, Hylleraas [4] and Hartree [5] set the foundation for the later work done in the field. Hylleraas introduced a framework to describe the arrangement of the electrons relative to the nucleus, as well as suggesting the form of the trial wave functions to be of the form

$$\Psi(\mathbf{r}_1, \mathbf{r}_2) = \sum_{i,j,k} a_{i,j,k} r_1^i r_2^j r_{12}^k e^{-\alpha r_1 - \beta r_2} \pm \text{exchange} \quad (1.12)$$

to represent the correlated form of the S states. Since then, much work has been done calculating the various properties of the helium atom, and the framework has



expanded considerably, reducing two-electron matrix elements into a series of radial integrals and angular momentum algebra done by Drake [6]. Further analysis finds this theory extended to lithium and lithium-like ions; work done by Yan, Tambasco and Drake [7] features calculations of energies of the lithium  $1s^22s^2S$  and  $1s^22p^2P$  isoelectronic sequences, as well as the oscillator strengths for the transition between the same two states. Further applications to this computational technique has also been applied to calculating the quenching rate for metastable singlet helium atoms and helium-like ions in addition to dipole polarizabilities and oscillator strength sums [8]. Work has also been done in comparing experimental results with theoretical calculations of the energies of  $2s2s^1S$  and  $2s2p^1P$  resonances of helium [9]. Other comparisons with experimental data both confirmed the theoretical techniques and provided asymptotic analysis that suggested revisions to the theoretical treatment of the quantum defect term used in the analysis of experimental data [10]. Use of variational wave functions, with Hylleraas-type basis sets have been used to calculate oscillator strengths in neutral helium [11]. Alternative methods include using variational Monte Carlo methods and correlated trial wave functions to calculate lowest-order relativistic corrections [12]. This work will contribute to the relativistic corrections for allowed transitions and provide a direct connection to the one-electron case using pseudostates to perform sums over intermediate states.

# Chapter 2

## Introduction

### 2.1 Dirac Relativistic Theory

The Dirac equation provides a fully covariant relativistic theory of radiative transitions in terms of the Dirac  $\alpha$ . A form of the interaction for the case of one-electron atoms, making the usual substitution for electromagnetic potentials yields

$$[E - e\Phi - \alpha \cdot (c\mathbf{p} - e\mathbf{A}) - \beta mc^2] \psi = 0 \quad (2.1)$$

where  $\Phi$  is the scalar potential and  $\mathbf{A}$  is the vector potential for the emitted or absorbed photon. This Dirac equation can be used to provide a covariant relativistic description of radiative transitions in terms of the Dirac  $\alpha \cdot A$  interaction for the case of one-electron atoms.

### 2.2 Applications to Many-Electron Atoms

For the case of many-electron atoms, there is no analytic Dirac equation like the one-electron atom case. One can either

- find approximate relativistic wave functions with the  $\alpha \cdot A$  form of the interac-

tion, similar to the Dirac form, or

- apply the Foldy-Wouthuysen transformation [13] to the  $\alpha \cdot A$  operator to obtain equivalent nonrelativistic operators that can be used with solutions to the nonrelativistic Schrödinger equation.

In its general form, these options can be expressed in the relation

$$\langle \psi_i^D | \alpha \cdot \mathbf{A} | \psi_f^D \rangle = \langle \psi_i^S | T^S | \psi_f^S \rangle \quad (2.2)$$

where the  $\psi^D$  are the Dirac wave functions and the  $\psi^S$  are the Schrödinger wave functions. Further, the Schrödinger operator  $T^S$  can be expressed as

$$T^S = T_0 + \alpha^2 T_2 + \dots \quad (2.3)$$

as the equivalent nonrelativistic transition operator correct up to some fixed order in powers of the fine structure constant  $\alpha$ .

Both options have their strengths and weaknesses. The first option described above is best for large values of the nuclear charge  $Z$  where relativistic effects dominate over electron correlation effects. The second option is preferable for low values of  $Z$  such as helium or lithium since the electron correlation effects can be more accurately described within the Schrödinger picture, and relativistic effects are relatively small. These relations can be understood intuitively by studying the critical expansion parameter  $(\alpha Z)^2$ .

Past work in this area has extensively studied the role that relativistic corrections plays for “forbidden” transitions, where the lowest-order relativistic corrections turn the forbidden transition into an allowed one. Such examples are the spin-forbidden electric dipole (E1) transition  $1s2p \ ^3P \rightarrow 1s^2 \ ^1S$  or the relativistic magnetic dipole transition  $1s2s \ ^3S \rightarrow 1s^2 \ ^1S$  which are available in the literature [2] [14].

In contrast, relatively little work has been done on relativistic corrections to ordinary allowed transitions such as  $1s2p\ ^2P \rightarrow 1s^2\ ^1S$ . In this case, the leading relativistic correction is the next-to-leading term  $\alpha^2 T_2$  in the transition matrix element as shown above.

Given this background, the purpose of this work is to perform high precision variational calculations for the relativistic corrections for the case of allowed E1 transitions, and to compare with known results for the one-electron case in the limit of large  $Z$ . In this limit, it is only the leading hydrogenic term in a  $1/Z$  expansion of  $T_2$  that contributes, and so a direct check is possible. The calculation involves the use of pseudostates to perform perturbation sums over complete sets of intermediate states. An important part of this work is to provide a test of these perturbation techniques.

This work will start with an analysis of the mathematical framework used to calculate atomic properties of the simplest system we have available. The two-body system of hydrogen provides a natural starting point that serves as both an entry to the techniques used, as well as a valuable check for further work, expanding to larger and more complicated systems. Even though helium only has one extra electron, this addition makes the problem much more difficult to solve. In fact, it can not be solved analytically in the way that hydrogen can. The techniques used to solve this problem will be examined, followed by corrections added to account for relativistic effects. Finally, the results of these calculations are presented, starting with the numerical stability, and then expanding the calculations with nuclear charge for the purpose of comparison with the hydrogenic results. This provides a direct check of the relativistic effects.

# Chapter 3

## Mathematical Models for Atomic Systems

### 3.1 Nonrelativistic Hydrogen

Before discussing the formulation and mathematical techniques for helium, it is informative to first discuss the simpler case of hydrogen. Starting with the simpler case allows for valuable insight into the mechanics of approximate variational solutions without extra weight or complexity of solving a three-body problem.

It is possible and instructive to start with an analogue to the hydrogen atom since it is a simple structure. A hydrogen atom is comprised of an electron orbiting a nucleus made up of a proton. In the corresponding problem from celestial mechanics, two bodies with masses  $m_1$  and  $m_2$  orbiting each other can be described by Newton's Law of Gravity, so the gravitational potential energy is

$$V_G(r) = -\frac{Gm_1m_2}{r} \quad (3.1)$$

where  $G$  is Newton's universal constant of gravitation, the minus sign accounts for the attraction, and  $r = |\mathbf{r}_1 - \mathbf{r}_2|$  is the distance between the two bodies [15]. Converting

to electrostatic units for the corresponding atomic problem, the potential becomes

$$V(r) = \frac{q_1 q_2}{r} \quad (3.2)$$

where  $q_1$  and  $q_2$  are the charges [16]. The electron charge can be set as  $q_1 = -e$  and the charge of the nucleus can be set as  $q_2 = Ze$ , which modifies the potential to now be

$$V(r) = -\frac{Ze^2}{r} \quad (3.3)$$

Having defined our potential, the next natural step is to find the energy, which for conservative systems is the same as the Hamiltonian  $H$ , so we can write  $H = T + V$ . Here  $T$  is defined in terms of the canonical momenta  $p_1$  and  $p_2$ , and is written as

$$T = \frac{p_1^2}{2m_1} + \frac{p_2^2}{2m_2} \quad (3.4)$$

We can now combine these pieces into the Hamiltonian as described earlier to obtain

$$H = T + V = \frac{p_1^2}{2m_1} + \frac{p_2^2}{2m_2} - \frac{Ze^2}{r} \quad (3.5)$$

making the substitution for the momentum operators [17]. Since this is a two-body problem, we have the option to simplify by switching to centre of mass plus relative coordinates. Note that the potential is already defined in terms of the relative coordinate. We define these quantities as

$$\mathbf{r} = \mathbf{r}_1 - \mathbf{r}_2 \quad \mathbf{R} = \frac{m_1 \mathbf{r}_1 + m_2 \mathbf{r}_2}{m_1 + m_2} \quad (3.6)$$

We can make similar changes to mass by defining  $M = m_1 + m_2$  as the total mass and  $\mu = \frac{m_1 m_2}{M}$  as the reduced mass. Redefine our momenta in terms of relative and

center-of-mass coordinates to obtain

$$\begin{aligned}
 \mathbf{P}_{cm} &= M\mathbf{V}_{cm} & \mathbf{p} &= \mu\mathbf{V}_{\mu} \\
 \mathbf{P}_{cm} &= m_1\mathbf{v}_1 + m_2\mathbf{v}_2 & \mathbf{p} &= \frac{m_1m_2}{m_1 + m_2}(\mathbf{v}_1 - \mathbf{v}_2) \\
 \mathbf{P}_{cm} &= M\mathbf{V}_{cm} & \mathbf{p} &= \frac{m_2\mathbf{p}_1 - m_1\mathbf{p}_2}{m_1 + m_2}
 \end{aligned}$$

which can be rearranged into a more usable form

$$\mathbf{p}_1 = \frac{m_1}{M}\mathbf{P}_{cm} + \mathbf{p} \qquad \mathbf{p}_2 = \frac{m_2}{M}\mathbf{P}_{cm} - \mathbf{p} \qquad (3.7)$$

Since  $V(r)$  is independent of  $R$ ,  $R$  is an ignorable coordinate, allowing us to set  $\mathbf{P}_{cm} = 0$ , yielding the Hamiltonian

$$H = \frac{p^2}{2\mu} - \frac{Ze^2}{r} + \frac{\mu}{M}p_1 \cdot p_2 \qquad (3.8)$$

At this point we have reduced a two-body problem to its equivalent one-body problem with relative coordinates and reduced mass  $\mu$ . We started here by referencing only the classical attraction between two bodies, but now it is time to include the quantum mechanical aspect of these bodies by factoring in the wave nature of matter. We do this by first making a substitution of canonical momentum for its operator form

$$\mathbf{p} \rightarrow \frac{\hbar}{i}\nabla \qquad (3.9)$$

and invoking Schrödinger's equation

$$H\psi(\mathbf{r}) \equiv \left( -\frac{\hbar^2}{2\mu}\nabla^2 - \frac{Ze^2}{r} \right) \psi(\mathbf{r}) = E\psi(\mathbf{r}) \qquad (3.10)$$

we obtain the second-order differential equation that now describes the probability amplitude  $\psi$  of finding an electron in a given volume. The associated boundary condition is  $\psi(\mathbf{r}) \rightarrow 0$  as  $r \rightarrow \infty$ , which leads to the discrete solutions that correspond to the discrete energy levels  $E$  of a hydrogen atom.

$$E_n = \frac{\mu Z^2 e^4}{\hbar^2} \left( \frac{-1}{2n^2} \right) \quad (3.11)$$

This result is the Rydberg formula for the energy levels of a hydrogen atom or similarly hydrogenic ion with nuclear charge  $Ze$  and principal quantum number  $n$ . Note that the energy is independent of the orbital angular momentum  $l$  and the magnetic quantum number  $m$ .

The energy levels correspond to the eigenvalues, which are accompanied by the eigenfunctions that have the form

$$\psi_{nlm}(r) \propto R_{nl} \left( \frac{Zr}{a_\mu} \right) \exp \left( -\frac{Zr}{na_\mu} \right) Y_l^m(\theta, \phi) \quad (3.12)$$

where  $a_\mu$  is the reduced Bohr radius, which effectively splits the wave function of the electron into two parts; the angular part and the radial part. The angular part is represented by a spherical harmonic  $Y_l^m(\theta, \phi)$  where  $\theta$  and  $\phi$  are the polar angles of the electron. The radial part is represented by a radial function  $R_{nl}$  which is given by

$$R_{nl}(\rho) = \rho^l {}_1F_1(-(n-l-1); 2l+2; 2\rho) \quad (3.13)$$

The radial function here is generated by a confluent hypergeometric function  ${}_1F_1(a; b; z)$  that gives a finite polynomial of order  $(n-l-1)$ . Note that the general form of having polynomials in  $r$  multiplied by exponentials is the pattern will be repeated in future chapters.



## 3.2 Nonrelativistic Helium

Now we approach the much more difficult problem of describing the helium atom. The difference between this case and the case of hydrogen is very significant; the addition of another electron, making this a three-body problem. There exists no solution to the three-body problem, in either classical or quantum mechanics. What we do instead is generate a sequence of approximate numerical solutions that converge to the exact answer. In this section we will look at this technique in greater depth, and discuss the high-precision variational methods that are used to generate solutions that are essentially, for all practical purposes, exact.

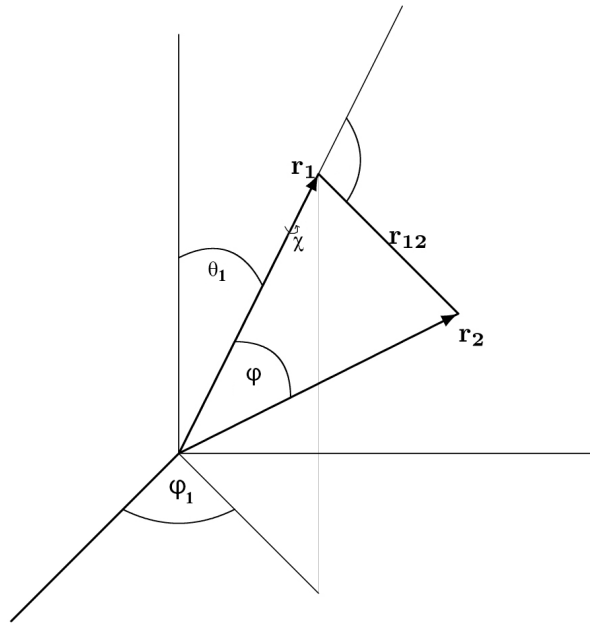


Figure 3.1: Hylleraas coordinate system for a helium atom with the nucleus at the origin.

It is instructive to establish our coordinate system visually. The figure above illustrates the relative coordinates, where  $r_1$  and  $r_2$  are the position vectors relative to the nucleus and  $r_{12}$  is the distance between the two electrons. We can adjust our

Hamiltonian from earlier to get

$$\left[ -\frac{\hbar^2}{2\mu} \left( \nabla_1^2 + \nabla_2^2 + 2\frac{\mu}{M} \nabla_1 \cdot \nabla_2 \right) - \frac{Ze^2}{r_1} - \frac{Ze^2}{r_2} - \frac{e^2}{r_{12}} \right] \Psi(\mathbf{r}_1, \mathbf{r}_2) = E\Psi(\mathbf{r}_1, \mathbf{r}_2) \quad (3.14)$$

which is the full Schrödinger equation in the center-of-mass frame. We now include a new term  $2\frac{\mu}{M}\nabla_1 \cdot \nabla_2$  known as the mass polarization term. This term accounts for the recoil of the nucleus due to the motion of the electrons. However, this term can be neglected in the limit where the mass of the nucleus  $M \rightarrow \infty$ . While this is a convenient choice, its not a precise one, so for our purposes it is essential to consider it as a small perturbation. Another addition to this Schrödinger equation is the  $\mathbf{r}_{12} = |\mathbf{r}_1 - \mathbf{r}_2|$  term that relates the distance between the two electrons. This term is what makes helium so much more complicated than hydrogen. Without this term the equation is separable and we could solve for wave functions in the same way that we did for hydrogen, as in (3.12). Even though we don't currently have exact solutions, we have several methods of approximation, namely the Hartree-Fock approximation, configuration interaction methods, and many-body perturbation theory. However, these methods are not accurate enough for our purposes.

### 3.2.1 Correlated Variational Basis Sets

Now that we know why we need better tools, it is time to discuss the tools that we are going to use. We will initially concern ourselves with the nonrelativistic Schrödinger equation, with a nucleus of infinite mass. Note here that this is a preliminary step, and we will be adding in relativistic corrections and finite nuclear mass later. Converting to atomic units, with  $e = \hbar = m = 1$ , the Schrödinger equation is then given by

$$\left( -\frac{1}{2}\nabla_1^2 - \frac{1}{2}\nabla_2^2 - \frac{Z}{r_1} - \frac{Z}{r_2} - \frac{1}{r_{12}} \right) \Psi(\mathbf{r}_1, \mathbf{r}_2) = E\Psi(\mathbf{r}_1, \mathbf{r}_2) \quad (3.15)$$

As referenced earlier, the simpler methods of theoretical atomic physics are not sufficiently accurate for our purposes. The technique proposed by Hylleraas in 1929 was to use the Rayleigh-Ritz variational method to find approximate solutions to the Schrödinger equation that approach the exact ones. The first step is to construct a trial function that appears to generally resemble the exact solution. We include adjustable parameters that can be varied to optimize some quantity which is traditionally the energy. As was hinted at in previous sections, we know that we can describe the radial component of one-electron hydrogen with a sum of powers of  $r$  times exponentials. This technique however doesn't translate well to helium because it doesn't account for the correlation energy. An attempt can be made to adjust the functional form of the approximate trial function to include explicitly the  $r_{12}$  coordinate

$$\Psi(\mathbf{r}_1, \mathbf{r}_2) = \sum_{i,j,k} a_{ijk} r_1^i r_2^j r_{12}^k e^{-\alpha r_1 - \beta r_2} Y_{l_1 l_2 L}^M(\hat{\mathbf{r}}_1, \hat{\mathbf{r}}_2) \quad (3.16)$$

where the quantities here match the physical definitions illustrated in 3.1, and  $Y_{l_1 l_2 L}^M(\hat{\mathbf{r}}_1, \hat{\mathbf{r}}_2)$  is the a vector coupled product of spherical harmonics, which will be dealt with in a later section. The coefficients  $a_{ijk}$  are known as linear variational parameters, and  $\alpha$  and  $\beta$  are known as nonlinear variational parameters that physically correspond to the distance scale for their respective radial components for the wave function. With this established, the next step is to limit the powers of  $r$  within a Pekeris shell such that  $i + j + k \leq \Omega$ , where  $\Omega$  is an integer. Given this limitation, there are then  $N = \frac{(\Omega+1)(\Omega+2)(\Omega+3)}{6}$  distinct terms. Table 2.1 demonstrates an example of this for 10 basis set functions. Here  $p$  represents a reference to a triplet of powers  $i, j, k$  that are in Eq. 3.16. For example, the first triplet referenced by  $p = 1$  corresponds to  $i = j = k = 0$ . With a set of integer powers, one can regard the function that is produced as a trial function which is a solution to the Schrödinger equation 3.15 with linear variational parameters  $a_{ijk} \equiv a_p$  and nonlinear variational parameters  $\alpha$  and  $\beta$ . Now we optimally choose these parameters based on a chosen criterion, which

$p$	$\Omega$	$i$	$j$	$k$
1	0	0	0	0
2	1	1	0	0
3	1	0	1	0
4	1	0	0	1

Table 3.1: Example of basis set for the case  $\Omega = 0$  and 1

we choose to be the energy. If we choose our trial function to have the general form  $\Psi_{tr} = \sum_{i=1}^N c_i \phi_i$  then we can calculate the expectation value of the Hamiltonian to be

$$E_{tr} = \frac{\langle \Psi_{tr} | H | \Psi_{tr} \rangle}{\langle \Psi_{tr} | \Psi_{tr} \rangle} = \langle \Psi_{tr} | H | \Psi_{tr} \rangle \quad (3.17)$$

where  $\Psi_{tr}$  is assumed normalized to unity. Using that fact, we can find an expression for the coefficients  $c_i$  by evaluating the expectation value

$$\begin{aligned} \langle \Psi_{tr} | \Psi_{tr} \rangle &= \sum_{ij} \langle c_i \phi_i | c_j \phi_j \rangle \\ &= \sum_i |c_i|^2 \\ &= |c_0|^2 + |c_1|^2 + \dots = 1 \end{aligned} \quad (3.18)$$

where  $c_i$  and  $\phi_i$  are the coefficients and the wave functions that make up the trial function. Using this expression, we can see that, with some work, the trial energy

takes the form

$$\begin{aligned}
E_{tr} &= \langle \Psi_{tr} | H | \Psi_{tr} \rangle \\
&= \sum_{ij} \langle c_i \phi_i | H | c_j \phi_j \rangle \\
&= \sum_i [\langle c_i \phi_i | H | c_0 \phi_0 \rangle + \langle c_i \phi_i | H | c_1 \phi_1 \rangle + \dots] \\
&= \sum_i [c_i^* c_0 \langle \phi_i | H | \phi_0 \rangle + c_i^* c_1 \langle \phi_i | H | \phi_1 \rangle + \dots] \\
&= \sum_i c_i^* [c_0 E_0 \langle \phi_i | \phi_0 \rangle + c_1 E_1 \langle \phi_i | \phi_1 \rangle + \dots] \\
&= c_0^* c_0 E_0 + c_1^* c_1 E_1 + \dots \\
&= |c_0|^2 E_0 + |c_1|^2 E_1 + \dots \\
&= (1 - |c_1|^2 - |c_2|^2 - \dots) E_0 + |c_1|^2 E_1 + \dots \\
E_{tr} &= E_0 + |c_1|^2 (E_1 - E_0) + |c_2|^2 (E_2 - E_0)
\end{aligned} \tag{3.19}$$

where we have used the assumption of  $\Psi_{tr}$  normalizing to unity to find this equation. Looking at the energy differences, all the terms after  $E_0$  are positive, due to each successive energy level being higher than the last. This makes it obvious that  $E_{tr} \geq E_0$  and thus, the trial energy provides an upper bound to the ground state energy.

With this we can vary both the linear and nonlinear parameters to obtain a minimum in the trial energy. Since the trial energy can never fall below the ground state energy, we know that minimum in the energy corresponds to the optimal parameters. This process of variational minimization corresponds to solving the system of equations  $\frac{\partial E_{tr}}{\partial c_i} = 0$  where  $c_i$  represents all of the linear and nonlinear parameters that are being varied.

Although the idea of a minimum energy  $E_{tr}$  being an upper bound is a well known idea, what is less well known is the Hylleraas-Undheim-McDonald theorem [18] which states that its not just the lowest-lying eigenvalue that is bounded by the minimized

trial eigenvalue; in fact all higher-lying variational eigenvalues are upper bounds to their corresponding exact energies. This can be seen in Figure 3.2, where the  $\lambda_N$  are the trial eigenvalues, which all lie above their respective energies. As the size of the basis set increases, the new eigenvalues  $\lambda_N$  interleave the previous set  $\lambda_{N-1}$ . As can be visually seen, these trial energies move downwards as  $N$  increases, eventually reaching their corresponding energy level in the limit  $N \rightarrow \infty$ . Thus,  $\lambda_N \geq E_N$  for finite  $N$ .

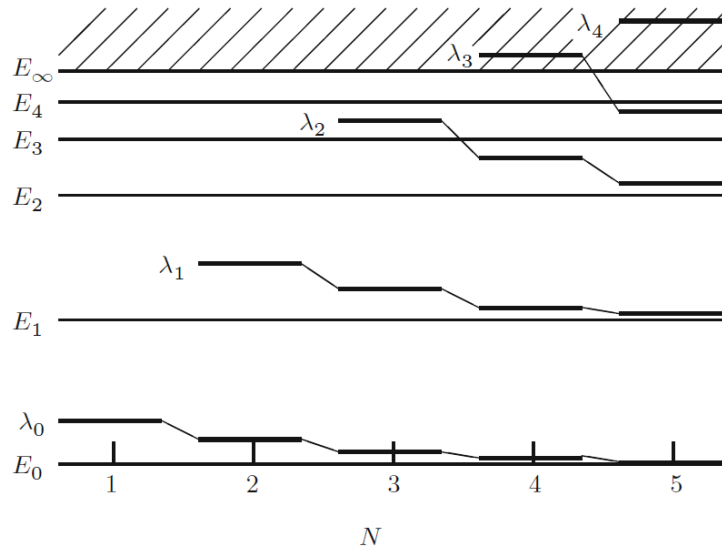


Figure 3.2: Hylleraas-Undheim-Macdonald Theorem, also known as the interleaving theorem [1]

The linear parameters  $c_i$  are relatively easy to solve for; essentially a system of  $N$  linear homogeneous algebraic equations that is equivalent to solving an  $N$ -dimensional generalized eigenvalue problem.

Optimization of the nonlinear parameters  $\alpha$  and  $\beta$ , is more difficult because the minimization conditions

$$\begin{aligned} \frac{\partial E_{tr}}{\partial \alpha} &= 0 \\ \frac{\partial E_{tr}}{\partial \beta} &= 0 \end{aligned} \tag{3.20}$$

are transcendental equations that cannot be solved algebraically, and are instead solved iteratively to find the minimum of the energy as one varies  $\alpha$  and  $\beta$ . Practically, this equates to finding a minimum in the energy by systematically varying parameters. Finding these variational parameters is the last element required to construct a trial wave function, in the form shown in Eq.3.16.

### 3.2.2 Evaluating Matrix Elements

All the matrix elements that we will need to evaluate are of the form

$$\langle \Psi'(\mathbf{r}_1, \mathbf{r}_2) | T_K^Q(\mathbf{r}_1, \mathbf{r}_2) | \Psi(\mathbf{r}_1, \mathbf{r}_2) \rangle \quad (3.21)$$

where  $T_K^Q$  is a tensor operator of rank  $K$  and component  $Q$ . With our assumed form for the wave functions, this can be written as a six-dimensional integral

$$I = \int \int d\mathbf{r}_1 d\mathbf{r}_2 R'(r_1, r_2, r_{12}) Y_{l'_1 l'_2 L'}^{M'}(r_1, r_2) T_{k_1 k_2 K}^Q Y_{l_1 l_2 L}^M(r_1, r_2) R(r_1, r_2, r_{12}) \quad (3.22)$$

where  $R, Y_{l_1 l_2 L}^M$ , and  $T_{k_1 k_2 K}^Q$  are, respectively, the radial function, the angular function, and the tensor operator [19]. By definition the radial and angular components of the wave function are separable, and usefully so is the volume element. This six-dimensional volume integral can be converted to two three-dimensional radial and angular integrals, written as

$$\int \int d\mathbf{r}_1 d\mathbf{r}_2 = \int_0^{2\pi} d\phi \int_0^{2\pi} d\varphi_1 \int_0^\pi \sin\theta_1 d\theta_1 \int_0^\infty r_1 dr_1 \int_0^\infty r_2 dr_2 \int_{|r_1-r_2|}^{r_1+r_2} r_{12} dr_{12} \quad (3.23)$$

where  $r_1, r_2$ , and  $r_{12}$  are the radial components and  $\theta_1, \varphi_1$  are the polar angles of  $\mathbf{r}_1$ , and  $\chi$  is the angle of rotation of the  $r_1, r_2, r_{12}$  triangle about the  $\mathbf{r}_1$  direction (see 3.1 [1]). Here, the dependent variables are defined as  $\theta_2, \varphi_2$ .

## Angular Integrals

Note that  $\theta_2$  and  $\phi_2$  are not independent variables. The angular portion of the integral is

$$\int_0^{2\pi} d\chi \int d\phi_1 \int \sin \theta_1 d\theta_1 Y_{l_1 m_1}^*(\theta_1, \varphi_1) Y_{l_2 m_2}^*(\theta_2, \varphi_2) = 2\pi \delta_{l_1 l_2} \delta_{m_1 m_2} P_{l_1}(\cos \theta) \quad (3.24)$$

where  $P_l(\cos \theta)$  is a Legendre polynomial and  $\theta$  is the angle between  $\mathbf{r}_1$  and  $\mathbf{r}_2$  [1]. Note also that  $\cos \theta$  is expressed radially in the form

$$\cos \theta = \frac{r_1^2 + r_2^2 - r_{12}^2}{2r_1 r_2} \quad (3.25)$$

using cosine law. Note that the form of the angular components can be expressed in terms of radial variables. The angular integral over vector-coupled spherical harmonics is now

$$\int_0^{2\pi} d\chi \int d\phi_1 \int \sin \theta_1 d\theta_1 Y_{l_1 m_1}^*(\mathbf{r}_1, \mathbf{r}_2) Y_{l_2 m_2}^*(\mathbf{r}_1, \mathbf{r}_2) = \delta_{L'L} \delta_{M'M} \sum_{\Lambda} C_{\Lambda} P_{\Lambda}(\cos \theta) \quad (3.26)$$

where we have evaluated the angular quantum numbers in terms of  $3-j$  symbols, as shown below in Eq.3.27 [1].

$$C_{\Lambda} = \frac{1}{2} [(2l_1 + 1)(2l'_1 + 1)(2l_2 + 1)(2l'_2 + 1)]^{\frac{1}{2}} (-1)^{L+\Lambda} (2\Lambda + 1) \\ \times \begin{pmatrix} l'_1 & l_1 & \Lambda \\ 0 & 0 & 0 \end{pmatrix} \begin{pmatrix} l'_2 & l_2 & \Lambda \\ 0 & 0 & 0 \end{pmatrix} \begin{Bmatrix} L & l_1 & l_2 \\ \Lambda & l'_2 & l'_1 \end{Bmatrix} \quad (3.27)$$

The use of angular momentum algebra allows for the angular components of the wave functions to be calculated simply in terms of  $3-j$  and  $6-j$  symbols.



## Radial Integrals

As for the radial portion of the integral, the general form can be expressed in terms of powers of  $r$  and exponentials. Using this as a base, the general integral formula can be expressed as

$$\begin{aligned} I_0(a, b, c; \alpha, \beta) &= \langle r_1^a r_2^b r_{12}^c e^{-\alpha r_1 - \beta r_2} \rangle_{rad} \\ I_0^{log}(a, b, c; \alpha, \beta) &= \langle r_1^a r_2^b r_{12}^c \ln(r_{12}) e^{-\alpha r_1 - \beta r_2} \rangle_{rad} \end{aligned} \quad (3.28)$$

where  $I_0$  is the integral to be solved [1]. Given the powers of  $r$ , these integrals reduce to either simple algebraic expressions, or digamma functions  $\Psi(n) = -\gamma + \sum_{k=1}^{n-1} k^{-1}$  and hypergeometric functions  $F(a, b, c; z)$ . For example, with  $a \geq 1$ ,  $b \geq 1$ ,  $c \geq 1$ , the radial integral has the general form

$$I_0(a, b, c; \alpha, \beta) = \frac{2}{c+2} \sum_{i=0}^{\lfloor (c+1)/2 \rfloor} \binom{c+2}{2i+1} [F_{a+2i+2, b+c-2i+2}(\alpha, \beta) + F_{b+2i+2, a+c-2i+2}(\beta, \alpha)] \quad (3.29)$$

where

$$F_{p,q}(\alpha, \beta) = \begin{cases} \frac{q!}{(\alpha+\beta)^{p+1} \beta^{q+1}} \sum_{j=0}^q \frac{(p+j)!}{j!} \left(\frac{\beta}{\alpha+\beta}\right)^j & q \geq 0, p \geq 0 \\ \frac{p!}{\alpha^{p+q+2}} \sum_{j=p+q+1}^{\infty} \frac{j!}{(j-q)!} \left(\frac{\alpha}{\alpha+\beta}\right)^{j+1} & q < 0, p \geq 0 \\ 0^a & p < 0 \end{cases} \quad (3.30)$$

with unspecified variational parameters  $\alpha$  and  $\beta$  [1].

## 3.3 Relativistic Corrections

We now consider the relativistic corrections to not only the energies of helium-like atoms, which have been established previously, but to the less well-known transition probabilities as well. To begin, the relativistic corrections to the energy of a given state can be expressed as a power series expansion where the corrections are of order

$\alpha^2$ . To achieve this format we start with general perturbation theory, using the Breit interaction to perturb the ordinary Hamiltonian as described in Eq.3.14. General perturbations have the form

$$H = H_0 + gV \quad (3.31)$$

where  $V$  is the perturbation and  $g$  is a parameter that controls the strength of the perturbation [20]. Using this as a framework, we can choose our perturbation to be the Breit interaction which accounts for the various relativistic contributions in the atomic system. The Hamiltonian now is adjusted by these interactions, and can be expressed as

$$H = H_0 + H_1 + H_2 + \dots + H_6 \quad (3.32)$$

where the individual contributing Hamiltonians  $H_i$  are found to be

$$\begin{aligned} H_0 &= -eV + \frac{1}{2m}(p_1^2 + p_2^2) \\ H_1 &= -\frac{1}{8m^3c^2}(p_1^4 + p_2^4) \\ H_2 &= -\frac{e^2}{2(mc)^2 r_{12}} \left[ \mathbf{p}_1 \cdot \mathbf{p}_2 + \frac{\mathbf{r}_{12} \cdot (\mathbf{r}_{12} \cdot \mathbf{p}_1)\mathbf{p}_2}{r_{12}^2} \right] \\ H_3 &= \frac{\mu}{mc} \left\{ \left[ \boldsymbol{\xi}_1 \times \mathbf{p}_1 + \frac{2e}{r_{12}^3} \mathbf{r}_{12} \times \mathbf{p}_2 \right] \cdot \mathbf{s}_1 + \left[ \boldsymbol{\xi}_2 \times \mathbf{p}_2 + \frac{2e}{r_{12}^3} \mathbf{r}_{21} \times \mathbf{p}_1 \right] \cdot \mathbf{s}_2 \right\} \\ H_4 &= \frac{ie\hbar}{(2mc)^2} (\mathbf{p}_1 \cdot \boldsymbol{\xi}_1 + \mathbf{p}_2 \cdot \boldsymbol{\xi}_2) \\ H_5 &= 4\mu^2 \left\{ -\frac{8\pi}{3} (\mathbf{s}_1 \cdot \mathbf{s}_2) \delta^{(3)}(\mathbf{r}_{12}) + \frac{1}{r_{12}^3} \left[ \mathbf{s}_1 \cdot \mathbf{s}_2 - \frac{3(\mathbf{s}_1 \cdot \mathbf{r}_{12})(\mathbf{s}_2 \cdot \mathbf{r}_{12})}{r_{12}^2} \right]' \right\} \\ H_6 &= 2\mu [\mathcal{H}_1 \cdot \mathbf{s}_1 + \mathcal{H}_2 \cdot \mathbf{s}_2] + \frac{e}{mc} [\mathbf{A}_1 \cdot \mathbf{p}_1 + \mathbf{A}_2 \cdot \mathbf{p}_2] \end{aligned}$$

where

$$V = \frac{Ze}{r_1} + \frac{Ze}{r_2} - \frac{e}{r_{12}} + \varphi(r_1) + \varphi(r_2), \quad \mu = \frac{e\hbar}{2mc} \quad (3.33)$$

where  $\mu$  is the Bohr magneton, and where each Hamiltonian  $H_i$  corresponds to a specific characteristic of the model [21]. They are described according to Bethe and

Salpeter [21] and are as follows:

- $H_0$  is the ordinary nonrelativistic Hamiltonian.
- $H_1$  is the relativistic correction due to the variation of mass with velocity.
- $H_2$  is the relativistic correction to the interaction between the electrons, due to the retardation of the electromagnetic field of an electron.
- $H_3$  is the interaction between the spin magnetic moment and the orbital magnetic moment of the electrons (known as spin-orbit coupling).
- $H_4$  has no classical analogue, but is characteristic of the Dirac theory.
- $H_5$  is the interaction between the spin magnetic dipole moments of the two electrons.
- $H_6$  is the interaction with an external magnetic field (not considered for our purposes).

With this formulation, it is now a relatively straight forward matter to calculate the relativistic corrections using given operators. The next section covers the calculation of the contributions to the relativistic corrections from individual operators arising from the Breit interaction. These results are calculated such that each individual contribution from the perturbations to the initial states and the final states are separate. This is done not only for clarity but also for ease of comparison with hydrogenic values.

# Chapter 4

## Calculations

In this chapter, we will look at the results of using relativistically perturbed wave functions, with the dipole transition operator to calculate matrix elements. Perturbations are carried out using the pseudospectral method to sum over intermediate states, and their convergence is shown as the size of the intermediate basis set is enlarged. The individual contributions to the perturbation are shown separately, and compiled for a total relativistic correction to the transition probability of the  $1s^2\ ^1S - 1s2p\ ^2P$  transition. These calculations are then expanded and scaled for higher values of the nuclear charge  $Z$  for the purpose of comparing with the results for the one-electron case of hydrogen in the limit of large  $Z$  [22].

The quantity to be calculated is the matrix element expression

$$\begin{aligned} &= \langle \psi_{1s}^{(0)} \alpha^0 + \psi_{1s}^{(1)} \alpha^2 | z | \psi_{2p}^{(0)} \alpha^0 + \psi_{2p}^{(1)} \alpha^2 \rangle \\ &= \langle \psi_{1s}^{(0)} | z | \psi_{2p}^{(0)} \rangle \alpha^0 + \langle \psi_{1s}^{(1)} | z | \psi_{2p}^{(0)} \rangle \alpha^2 + \langle \psi_{1s}^{(0)} | z | \psi_{2p}^{(1)} \rangle \alpha^2 \\ &= \langle \psi_{1s}^{(0)} | z | \psi_{2p}^{(0)} \rangle \alpha^0 + \left[ \sum_n \frac{\langle \psi_{1s} | B | \psi_{ns} \rangle \langle \psi_{ns} | z | \psi_{2p} \rangle}{E_{1s} - E_{ns}} \right. \\ &\quad \left. + \sum_{n'} \frac{\langle \psi_{1s} | z | \psi_{n'p} \rangle \langle \psi_{n'p} | B | \psi_{2p} \rangle}{E_{2p} - E_{n'p}} \right] \alpha^2 \end{aligned} \tag{4.1}$$

where  $B$  is the perturbation which is, in this case, the terms from the Breit inter-

action. This matrix element consists of a series of matrix elements, from the many terms in the Breit interaction, calculated individually and then combined. Note that the terms considered in this work are limited to  $p^4, \delta(r_1), \delta(r_{12})$ , spin-orbit, spin-other-orbit, and magnetic spin-spin. The last three are often abbreviated as SO, SOO, and SS respectively. The first topic to discuss is the results for the individual contributions and their convergence proportional to the increasing dimension of the basis set. Next we will investigate at the results of scaling the calculations with an increasing nuclear charge  $Z$ , where the system retains its two-electron structure but the nucleus increases its number of protons, which physically corresponds to ions of higher  $Z$  atoms. This is done such that, in the limit  $Z \rightarrow \infty$ , the hydrogenic results are obtained. This provides a method to check and confirm the results obtained in this work by comparison with the results of Sami [22].

## 4.1 Pseudospectral Convergence

The sum over intermediate states is represented by summing over pseudostates that are generated as described in Section 3.2.1. Recall the visualization in Figure 3.2 where each successive basis set has the effect of “squeezing” the result between the previous result (calculated with the previous basis set) and the actual value. This applies only if the result is an upper or lower bound, such as the energy. Here the results converge to a specific value as the basis set increases in size. The results for each basis set used in this work and each individual contribution from the Breit interaction are tabulated in Tables 4.1 and 4.2. In Figures 4.1 and 4.2, it can be seen that the matrix elements for each relativistic contribution that is calculated each converge to a specific value as the basis sets get larger.

Table 4.1:  $\langle \psi_{1s}^{(1)} | z | \psi_{2p}^{(0)} \rangle$ , initial state relativistic contributions.

Basis Set Size	$p^4$	$\delta(r_1)$	$\delta(r_{12})$	SO	SOO	SS
182	-4.10336	-1.83656	-0.16289	0	0	0
236	-4.02783	-1.81759	-0.16180	0	0	0
302	-3.72709	-1.74130	-0.15985	0	0	0
376	-4.07448	-1.82869	-0.16058	0	0	0
464	-3.92545	-1.79084	-0.15926	0	0	0
561	-4.31443	-1.88900	-0.16098	0	0	0
674	-4.39148	-1.90865	-0.16171	0	0	0
797	-4.57257	-1.95326	-0.16030	0	0	0
938	-4.53328	-1.94348	-0.16039	0	0	0

Table 4.2:  $\langle \psi_{1s}^{(0)} | z | \psi_{2p}^{(1)} \rangle$ , final state relativistic contributions.

Basis Set Size	$p^4$	$\delta(r_1)$	$\delta(r_{12})$	SO	SOO	SS
104	-0.2769727020	0.1399664960	-0.0176706940	-0.6072900220	0	0
145	-0.2755234440	0.1401098920	-0.0176406420	-0.6072546980	0	0
197	-0.2754221720	0.1401120450	-0.0176323070	-0.6072444750	0	0
265	-0.2754883810	0.1401056830	-0.0176299790	-0.6072417910	0	0
346	-0.2756371950	0.1400975920	-0.0176292500	-0.6072410290	0	0
446	-0.2756386170	0.1400972850	-0.0176290240	-0.6072409390	0	0
559	-0.2756365330	0.1400972300	-0.0176289580	-0.6072408710	0	0
692	-0.2756402360	0.1400971040	-0.0176289320	-0.6072408730	0	0
836	-0.2756412830	0.1400970920	-0.0176289230	-0.6072408710	0	0

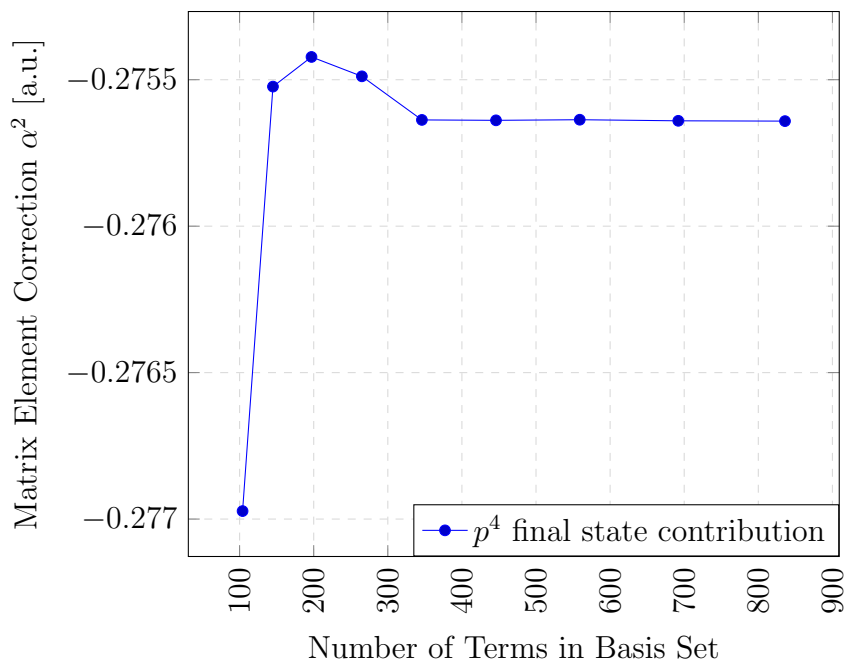


Figure 4.1: Convergence of  $p^4 1s2p^1P$  state perturbation contribution with increasing basis set size.

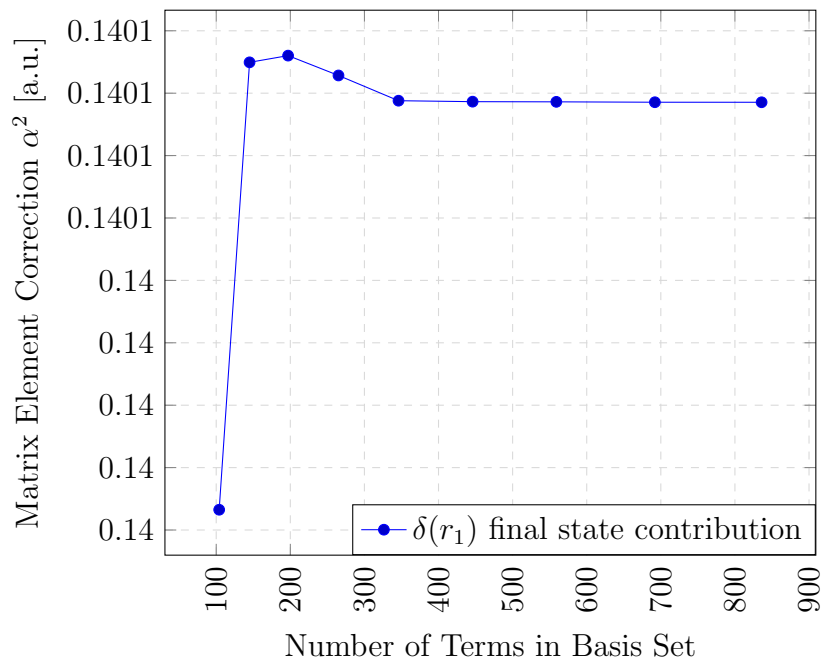


Figure 4.2: Convergence of  $\delta(r_1) 1s2p^1P$  state perturbation contribution with increasing basis set size.



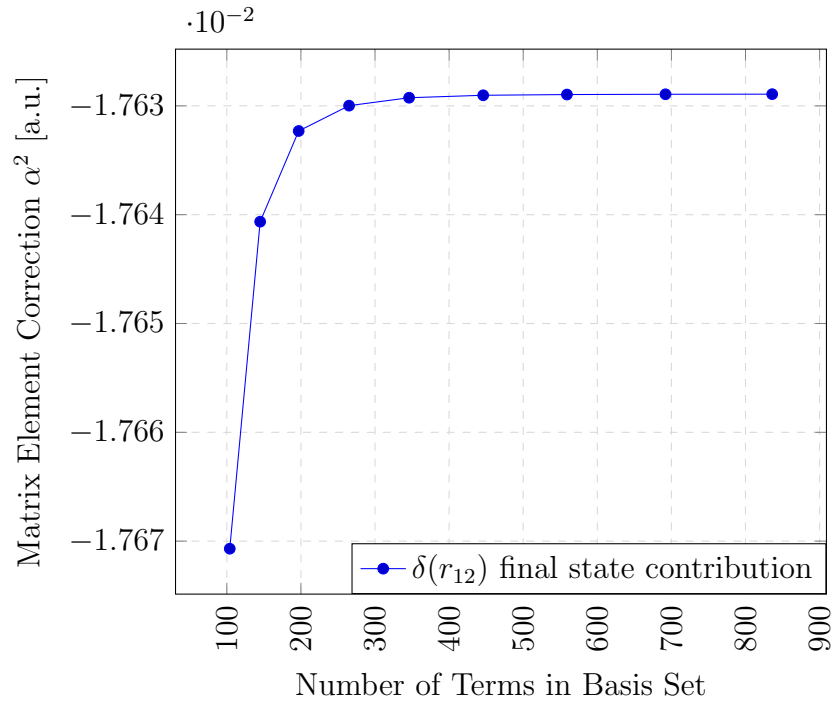


Figure 4.3: Convergence of  $\delta(r_{12})$   $1s2p$   $^1P$  state perturbation contribution with increasing basis set size.

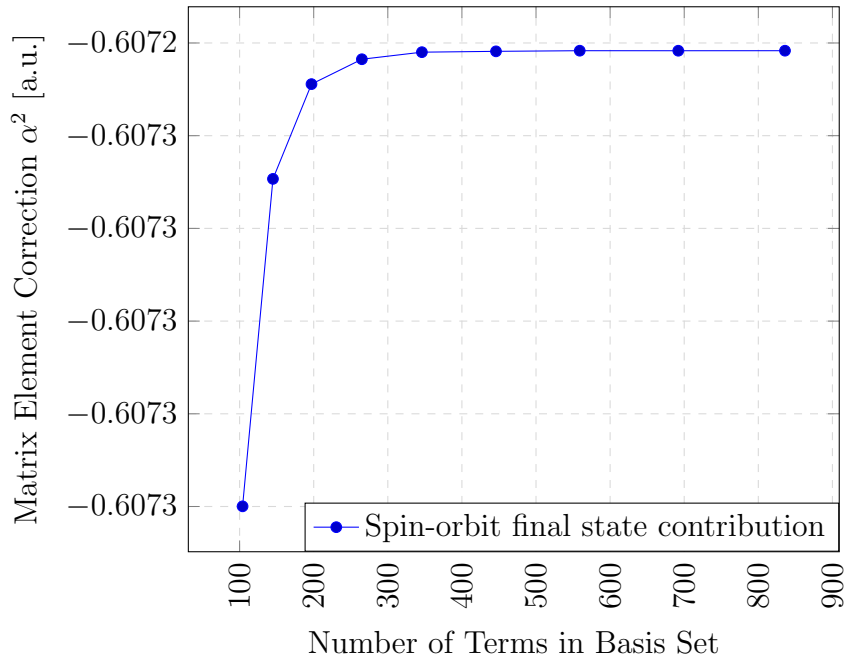


Figure 4.4: Convergence of spin-orbit  $1s2p$   $^1P$  state perturbation contribution with increasing basis set size.

Note that the values tabulated are purposefully not truncated to show precisely which figures converge. Now we look to the initial state contributions, the calculated values that corresponds to the matrix elements summed over intermediate S states, represented by the pseudospectral basis set. These values are displayed as their individual contributions, and for the initial S states, there are only two contributions from the Breit interaction. The first is the  $p^4$  matrix element contribution, and the second is the  $\delta(r_1)$  term, all others are zero.

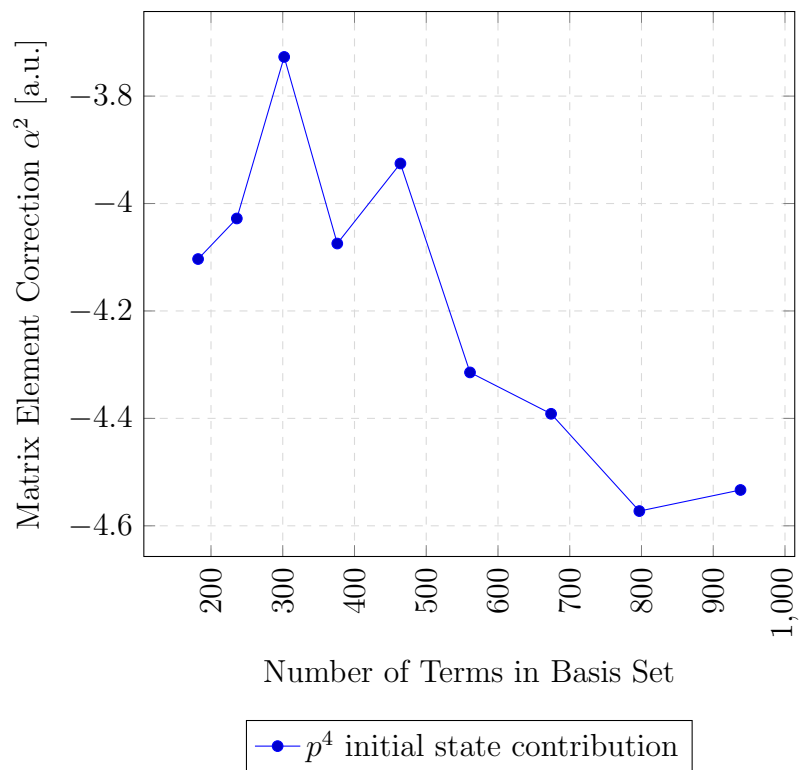


Figure 4.5: Convergence of  $p^4 1s^2 1S$  state perturbation contribution with increasing basis set size.

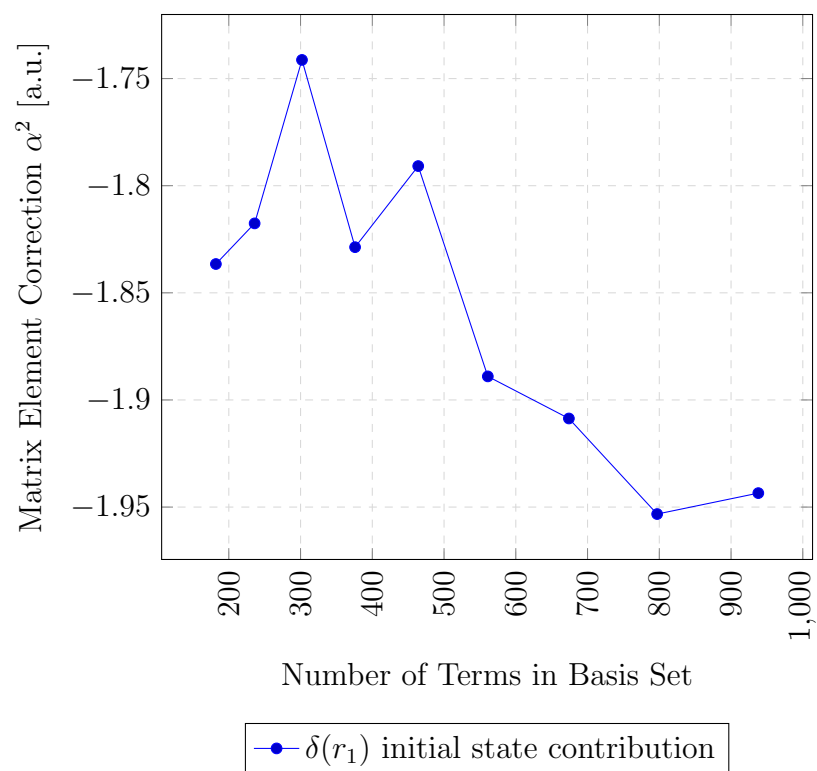


Figure 4.6: Convergence of  $\delta(r_1)$   $1s^2$   $^1S$  state perturbation contribution with increasing basis set size.

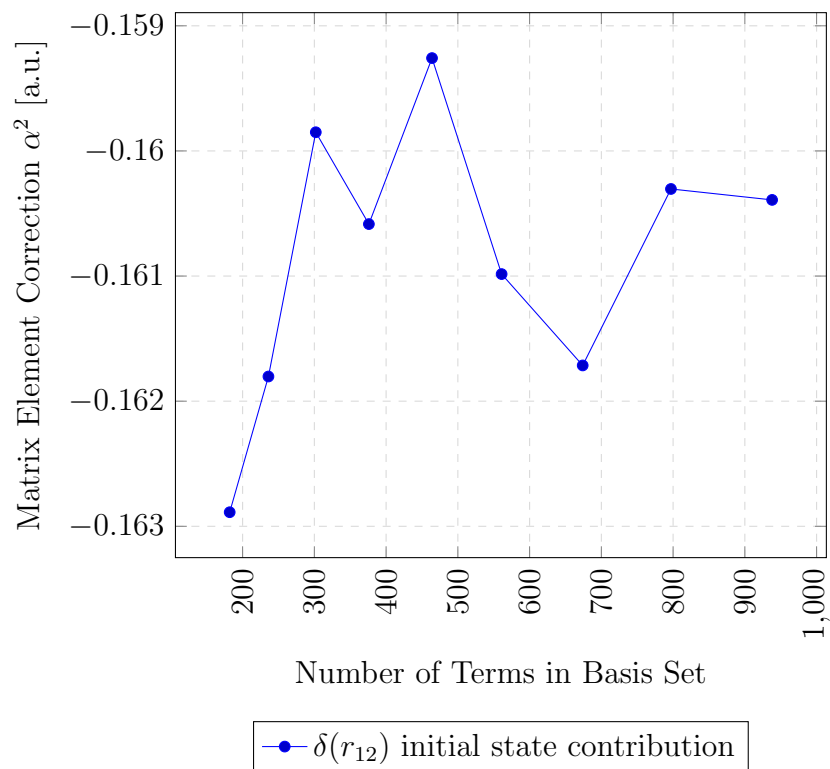


Figure 4.7: Convergence of  $\delta(r_{12})$   $1s^2$   $^1S$  state perturbation contribution with increasing basis set size.

As can be seen from above, while the final P state term contributions displays a trend of convergence, the initial S state terms appears rather nonconvergent. An explanation for this behavior is that this result is likely due to the singularity of the S states. While the P states go to zero at the origin, the S states diverge at the origin; meaning that their integrals result in a logarithmic term, which the current framework does not consider. For reference, the analytic normalized first order solutions to the perturbation equations are, using Cohen's [23] results and starting with the initial state  $p^4$  contribution,

$$\Psi_{1s}^{(1)} = \left( -\ln(2) - \ln(r) + \frac{1}{2r} - \frac{r}{2} + \frac{(-4\gamma + 7)}{4} \right) \Psi_{1s}^{(0)} \quad (4.2)$$

and for the  $\delta(r_1)$  contribution, the normalized first order wave function correction was determined to be

$$\Psi_{1s}^{(1)} = \left[ \frac{\ln(2)}{2} + \frac{\ln(r)}{2} - \frac{1}{4r} + \frac{r}{2} + \frac{(2\gamma - 5)}{4} \right] \Psi_{1s}^{(0)} \quad (4.3)$$

For the final state  $p^4$  contribution the first order wave function correction is

$$\Psi_{2p}^{(1)} = \frac{48 \ln(r)r - 72 + 3r^2 + (48\gamma - 97)r}{18r} \Psi_{2p}^{(0)} \quad (4.4)$$

where  $\gamma$  is the Euler-Mascheroni constant [22]. The trial wave functions outlined earlier do not consider logarithmic terms, and the programs currently do not support the inclusion of a logarithmic term, and so that factor is not represented in the calculations made in this work. This reasoning is consistent with the results for the final P states, which all converge individually as expected. It is valuable here to consider the scale at which this initial state terms exist. The plot in Figure 4.8 displays the convergence of all of the individual contributions to the relativistic corrections on the same axis.

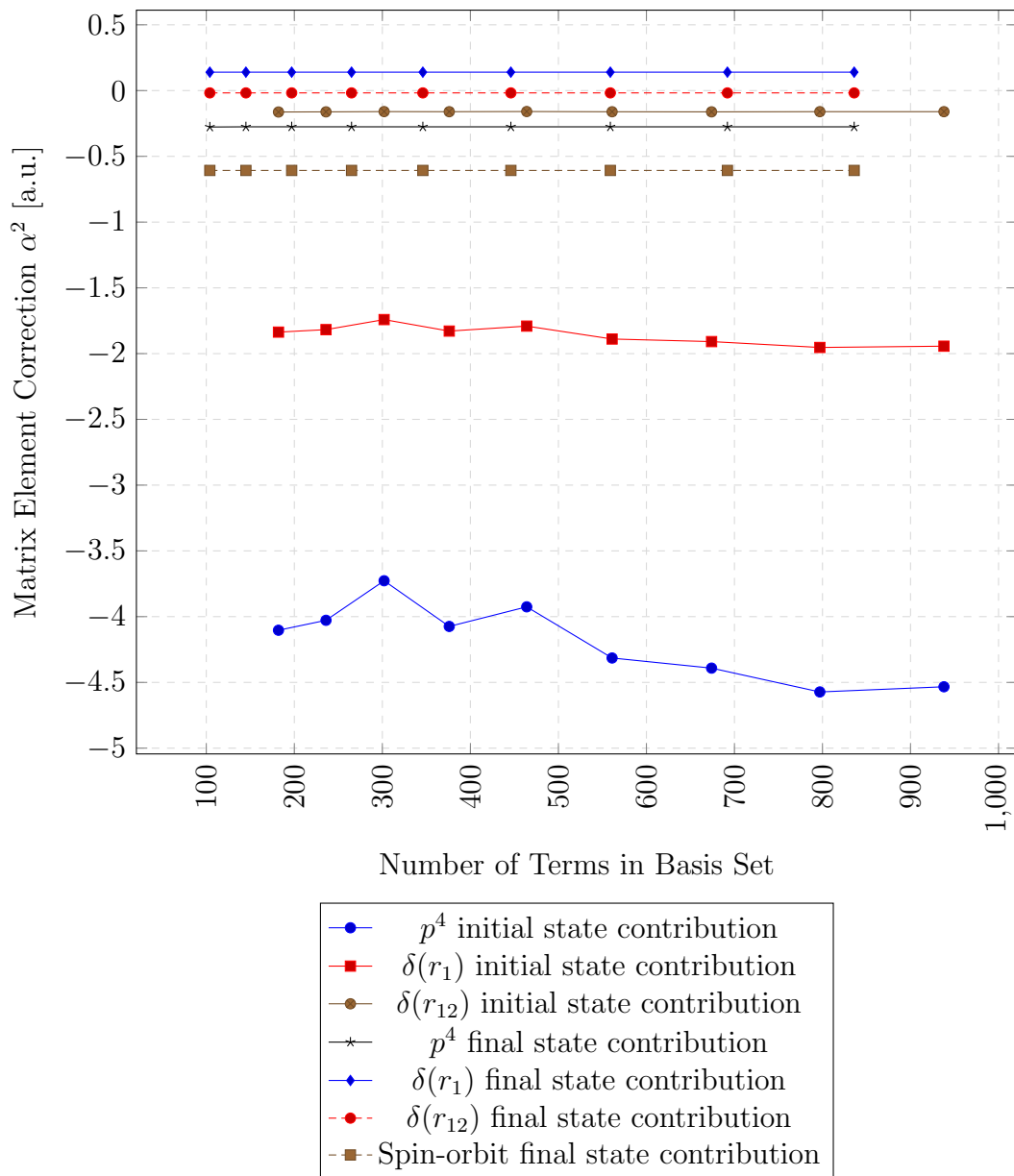


Figure 4.8: Comparative convergence of  $1s^2\ ^1S$  and  $1s2p\ ^1P$  state perturbation contributions.

Plotting these two quantities on the same graph highlights their relative importance and convergence, while considering the conditions affecting the contributions from the initial state.

Here, the nonrelativistic portions are factored out of the values such that what remains is the relativistic correction in the form  $1 + R\alpha^2$  where  $R$  is the relativistic correction. The individual contributions of each calculated matrix element of the relevant Breit interaction is tabulated in Tables 4.3 and 4.4.



Table 4.3:  $1s^2\ ^1S$  state contributions to the relativistic corrections to the transition probability, for the case of helium.

Contribution	Value $\alpha^0$	Value $\alpha^2$
Nonrelativistic	1	
$p^4$		-7.6(6)
$\delta(r_1)$		-3.27(7)
$\delta(r_{12})$		-0.2695(3)
Spin-Orbit		0
Spin Other-Orbit		0
Magnetic Spin-Spin		0

Table 4.4:  $1s2p\ ^1P$  state contributions to the relativistic corrections to the transition probability, for the case of helium.

Contribution	Value $\alpha^0$	Value $\alpha^2$
Nonrelativistic	1	
$p^4$		-0.46320(6)
$\delta(r_1)$		-0.004454(6)
$\delta(r_{12})$		-0.0296248(3)
Spin-Orbit		-1.02044865(6)
Spin Other-Orbit		0
Magnetic Spin-Spin		0

## 4.2 Nuclear Charge Scaling

In order to compare with Schrödinger wave functions and a relativistically corrected nonrelativistic operator, we first extend the calculations made for helium to higher values of nuclear charge  $Z$ , increasing the charge of the nucleus. This process maintains the two-electron structure while the nucleus gains more protons. The results are tabulated in Table 4.5; note that they are expressed in the second form shown at the beginning of this chapter, using the values calculated with the largest basis set used, and without their individual  $Z$ -scaling factored out.

Table 4.5: Nuclear charge  $Z$  scaling of the initial state contributions.

$Z$	2	3	4	5	6	7
Nonrelativistic	1	1	1	1	1	1
$p^4$	-7.66(5)	-5.44(1)	-4.16(6)	-3.39(9)	-2.85(9)	-2.44(2)
$\delta(r_1)$	-3.27(7)	-2.17(2)	-1.61(6)	-1.29(4)	-1.07(8)	-0.91(7)
$\delta(r_{12})$	-0.2695(3)	-0.189(7)	-0.146(9)	-0.1201(9)	-0.1016(7)	-0.0881(5)

$Z$	8	9	10	11	12	13
Nonrelativistic	1	1	1	1	1	1
$p^4$	-2.14(5)	-1.93(8)	-1.74(2)	-1.58(8)	-1.45(5)	-1.34(3)
$\delta(r_1)$	-0.80(1)	-0.72(2)	-0.64(6)	-0.58(3)	-0.53(5)	-0.49(3)
$\delta(r_{12})$	-0.0777(3)	-0.0703(7)	-0.0635(0)	-0.0574(8)	-0.0528(7)	-0.0489(8)

$Z$	14	15	16	17	18
Nonrelativistic	1	1	1	1	1
$p^4$	-1.25(1)	-1.16(9)	-1.09(7)	-1.03(3)	-0.97(6)
$\delta(r_1)$	-0.45(9)	-0.42(8)	-0.40(1)	-0.37(7)	-0.35(6)
$\delta(r_{12})$	-0.0456(1)	-0.0427(0)	-0.04015(7)	-0.03785(8)	-0.03583(5)

Table 4.6: Nuclear charge  $Z$  scaling of the final state contributions.

$Z$	2	3	4	5	6	7
Nonrelativistic	1	1	1	1	1	1
$p^4$	-0.4632(2)	-0.4007(6)	-0.3367(4)	-0.2893(8)	-0.2533(9)	-0.2251(8)
$\delta(r_1)$	-0.00445(4)	0.00706(6)	0.00888(1)	0.00781(6)	0.00645(5)	0.00528(8)
$\delta(r_{12})$	-0.029624(8)	-0.033091(1)	-0.030396(1)	-0.027056(8)	-0.024073(3)	-0.021565(3)
Spin-Orbit	-1.0204486(5)	-1.1555165(4)	-1.2070779(8)	-1.2310801(9)	-1.2439334(7)	-1.2515303(7)

$Z$	8	9	10	11	12	13
Nonrelativistic	1	1	1	1	1	1
$p^4$	-0.2025(2)	-0.1860(0)	-0.1699(1)	-0.1553(2)	-0.1440(8)	-0.1343(4)
$\delta(r_1)$	0.00435(3)	0.00367(1)	0.00309(9)	0.00261(4)	0.00225(4)	0.00196(2)
$\delta(r_{12})$	-0.019477(6)	-0.017930(7)	-0.016400(4)	-0.015001(8)	-0.013920(4)	-0.012981(1)
Spin-Orbit	-1.256356(8)	-1.2737351(6)	-1.2729122(9)	-1.2635010(8)	-1.2647236(3)	-1.2656555(5)

Z	14	15	16	17	18
Nonrelativistic	1	1	1	1	1
$p^4$	-0.1258(3)	-0.1183(3)	-0.1116(6)	-0.1057(7)	-0.1003(5)
$\delta(r_1)$	0.00172(2)	0.00152(2)	0.00135(6)	0.00121(4)	0.00109(4)
$\delta(r_{12})$	-0.012158(8)	-0.011431(5)	-0.010785(7)	-0.010208(2)	-0.009688(8)
Spin-Orbit	-1.2663798(3)	-1.2669523(2)	-1.2674113(7)	-1.2677840(0)	-1.2680900(8)

### 4.3 Comparisons with Schrödinger Technique

The comparison used in this work compares the technique outlined in this chapter, using relativistically corrected wave functions with a nonrelativistic operator, with exact analytic results in the one-electron case [22]. To make the connection between the two-electron helium system and the one-electron hydrogenic system, the first step is to scale the nucleus such that one is able to take the limit  $Z \rightarrow \infty$ . As an example, Figure 4.9 shows that calculated values asymptotically approach a definite value in the large- $Z$  limit.

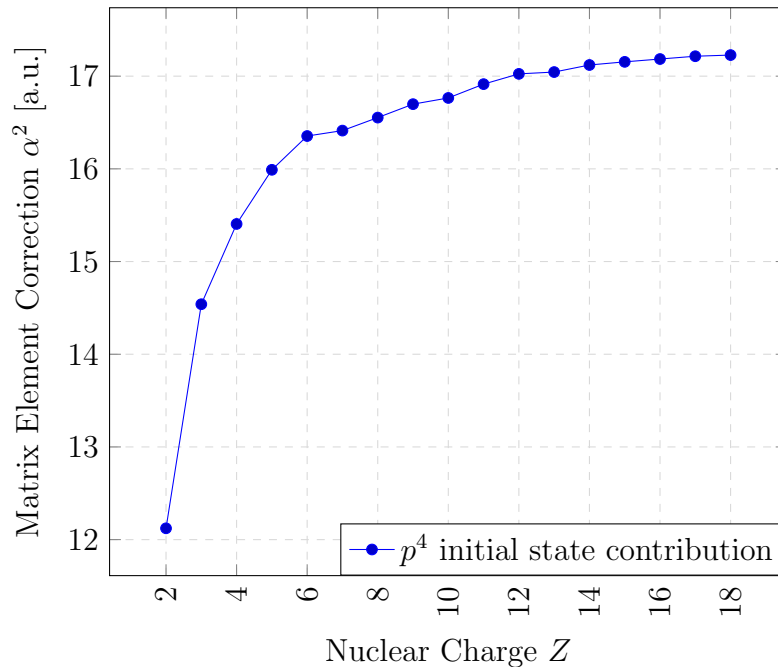


Figure 4.9:  $Z$  expansion of the  $p^4$  contribution from the initial state.

This is done for each individual contribution to the relativistic correction of order  $\alpha^2$ . When graphed against  $1/Z$ , what is obtained is an asymptotically straight line whose y-intercept corresponds to the value at the  $Z \rightarrow \infty$  limit. Further, each contribution has a different intrinsic  $Z$ -scaling which must be factored out before the values take a linear form in the graph, as shown in Figure 4.10.

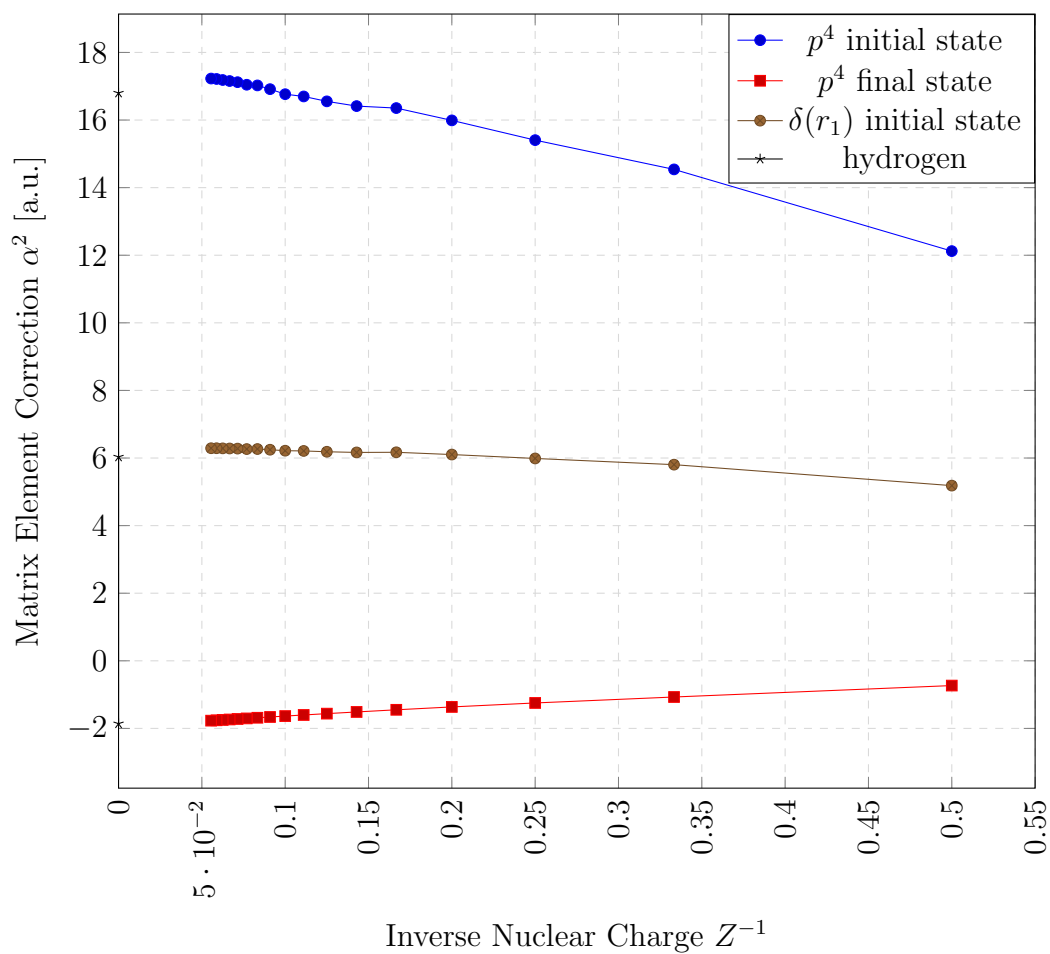


Figure 4.10:  $Z^{-1}$  expansion, with inherent  $Z$ -scaling factored out, to compare with hydrogenic values.

Table 4.7: Relativistic corrections to transition probability, in comparison with hydrogenic values.

Source	Nonrelativistic $\alpha^0$	$p^4$ initial state $\alpha^2$	$p^4$ final state $\alpha^2$	$\delta(r_1)$ initial state $\alpha^2$
This work	1	18	-1.94	6.35
Hydrogenic [22]	1	17	-1.86	6.03

The values in Table 4.7 are calculated by using the  $Z$ -scaled values, and removing  $Z$  dependence from each individual contribution to the  $\alpha^2$  relativistic correction. Note that they are presented in a form that removes the nonrelativistic portion such that a direct connection to the  $\alpha^2$  correction can be made, for example the contribution from the  $p^4$  in the final state can be expressed as

$$\langle \psi_{1s}^{(0)} | z | \psi_{2p}^{(1)} \rangle_{p^4} = T_{NR} \alpha^0 (1 - 1.94 \alpha^2) \quad (4.5)$$

where the  $\alpha^2$  term has the nonrelativistic portion factored out.



# Chapter 5

## Conclusion

In this thesis, we examined the basics of atomic theory starting with the Schrödinger equation and its application to one-electron hydrogenic atoms. Non-relativistically, it is possible to describe the electron wave functions as exact analytic solutions, as described. The same is not true when the system extends to two electrons, as in the case of helium and other two-electron systems. In general, when dealing with many-body systems, it is not possible to find exact analytic solutions although it is still possible to use specialized mathematical methods such as Hylleraas coordinates that can serve to represent the desired quantities to high accuracy. The technique used in this work was the pseudospectral method, using generated pseudostates to represent the sum over intermediate states that arises from perturbation theory used to calculate relativistic corrections to a nonrelativistic framework.

It was shown that when using this method, calculations converge to a well defined value, becoming more precise with larger basis sets that represent the infinite sum over intermediate states. Furthermore, the individual contributions that make up the relativistic corrections up to order  $\alpha^2$  were shown individually, to converge to a specific value. This process was then expanded to systems with a larger nuclear charge  $Z$ , by scaling the nuclear charge  $Z$ . This  $Z$ -scaling, while interesting in its

own right, was also useful in making an important comparison to the one-electron hydrogenic system. Taking the limit  $Z \rightarrow \infty$  should result in the hydrogenic results, and indeed this is the result that this work provides. Comparisons included only the relevant quantities that are relevant in the one-electron hydrogenic case, as some contributions calculated from helium have no context in the hydrogenic comparison. The result is an interesting one; the results that one obtains by applying the Foldy-Wouthuysen transformation to a nonrelativistic operator with nonrelativistic wave functions for the case of hydrogen [22] can also be obtained by  $Z$ -scaling the process outlined in this work done for helium. This connection provides a useful way to compare and confirm the results shown in this work.

Further work on this topic would include modifying the trial wave functions described in earlier sections to include a logarithmic term. As could be seen in earlier chapters, the singularity of the S states means that the integral over the origin results in a logarithmic term that is thus not well accounted for in the current formulation. This could also be improved by increasing the size of the basis set, although the computation time becomes increasingly restrictive. Current calculations take on the scale of days to complete all calculations over basis sets, and for each value of  $Z$  that this work considers in the nuclear charge scaling.

The results of this thesis therefore unify matrix elements obtained for two-electron atoms in the limit of high- $Z$  with those obtained by Sami [22] in the one-electron hydrogenic case directly from the Dirac equation, and from equivalent nonrelativistic operators.

# Appendix A

## The Breit Equation

We consider in this section a method to obtain eigenvalues in the form of an expansion in powers of  $\alpha$ , the fine structure constant which can be expressed in the relation

$$\alpha = \frac{e^2}{4\pi\epsilon_0\hbar c} \quad (\text{A.1})$$

revealing  $\alpha$  to be a dimensionless quantity that has a numerical value of  $1/137.035999139$ .

The Breit equation is a differential equation for a relativistic wave function  $\Psi$  for two electrons interacting with each other and an external electromagnetic field. In this way, the Breit equation is similar to the Dirac equation for one electron, but it differs in that the Breit equation is not Lorentz invariant [21]. The starting point here is

$$(E - H_{(1)} - H_{(2)} - \frac{e^2}{r_{12}})\Psi = -\frac{e^2}{2r_{12}} \left[ \alpha_1 \cdot \alpha_2 + \frac{(\alpha_1 \cdot \mathbf{r}_{12})(\alpha_2 \cdot \mathbf{r}_{12})}{r_{12}^2} \right] \Psi \quad (\text{A.2})$$

where

$$H_{(1)} = -e\phi(\mathbf{r}_1) + \beta_1 mc^2 + \alpha_1 \cdot (c\mathbf{p}_1 + e\mathbf{A}(\mathbf{r}_1)) \quad (\text{A.3})$$

and where  $\phi(\mathbf{r}_1)$  and  $\mathbf{A}(\mathbf{r}_1)$  are the scalar and vector potentials of the external electromagnetic field, including the nuclear Coulomb potential. The Breit equation is based on two different types of approximations. The first is that Eq.A.2 is only an

approximation to the relativistic interaction between the two electrons as well as their regular Coulomb interaction. While the right side of Eq.A.2 is consistent with one-electron Dirac theory, it is not compatible with Dirac pair theory, which will be the basis of the second approximation [21].

To discuss the implications of Dirac pair theory, it is more convenient to work in momentum space, so the Breit equation can be expressed as an integral equation in momentum space

$$\begin{aligned}
(E - H_{(01)} - H_{(02)})\Psi'(\mathbf{p}_1, \mathbf{p}_2) = & -e \int d^3k \{[\phi(-\mathbf{k}) - \alpha_1 \cdot \mathbf{A}(-\mathbf{k})] \Psi'(\mathbf{p}_1 + \mathbf{k}, \mathbf{p}_2) \\
& + [\phi(-\mathbf{k}) - \alpha_2 \cdot \mathbf{A}(-\mathbf{k})] \Psi'(\mathbf{p}_1, \mathbf{p}_2 + \mathbf{k})\} \\
& + \frac{e^2}{2/\pi i^2} \int \frac{d^3k}{k^2} (1 - \mathcal{B}) \Psi'(\mathbf{p}_1 - \mathbf{k}, \mathbf{p}_2 + \mathbf{k})
\end{aligned} \tag{A.4}$$

where

$$\begin{aligned}
H_{01} = mc^2\beta_1 + c\alpha_1 \cdot \mathbf{p}_1 \\
\mathcal{B} = \alpha_1 \cdot \alpha_2 - \frac{\alpha_1 \cdot \mathbf{k} \alpha_2 \cdot \mathbf{k}}{k^2}
\end{aligned} \tag{A.5}$$

where the momentum space wave function  $\Psi'$  is like the previous  $\Psi$ , in that it is a 16-component spinor that can be split into its constituent 4-component forms that arise from the “spin-up” and “spin-down” possibilities for each of the two electrons. It was shown by Bethe and Salpeter that the fine structure effects can be sufficiently obtained by considering the equation for only  $\Psi_+$ , and setting  $\Psi_-$  equal to zero [21]. Similarly, this approximation can be used for the two-electron case, where Eq.A.4 can be rewritten into four coupled integral equations of the Pauli spinor  $\Psi_{++}$ ,  $\Psi_{+-}$ ,  $\Psi_{-+}$ , and  $\Psi_{--}$ . Then, similar to the Dirac one-electron case, the  $\Psi_{+-}$ ,  $\Psi_{-+}$ , and

$\Psi_{--}$  components are set to zero, leaving only  $\Psi_{++}$ . This choice yields the equation

$$\begin{aligned}
[E - E(p_1) - E(p_2)] \Psi_{++}(\mathbf{p}_1, \mathbf{p}_2) = & -e \int d^3k \left\{ \left[ \phi(-\mathbf{k}) I_{++}^{(1)}(\mathbf{p}_1, \mathbf{p}_1 + \mathbf{k}) \right. \right. \\
& \left. \left. - \mathbf{A}(-\mathbf{k}) \cdot \alpha_{++}^{(1)}(\mathbf{p}_1, \mathbf{p}_1 + \mathbf{k}) \right] \Psi_{++}(\mathbf{p}_1 + \mathbf{k}, \mathbf{p}_2) \right. \\
& \left. + \left[ \phi(-\mathbf{k}) I_{++}^{(2)}(\mathbf{p}_2, \mathbf{p}_2 + \mathbf{k}) - \mathbf{A}(-\mathbf{k}) \cdot \alpha_{++}^{(2)}(\mathbf{p}_2, \mathbf{p}_2 + \mathbf{k}) \right] \Psi_{++}(\mathbf{p}_1, \mathbf{p}_2 + \mathbf{k}) \right\} \\
& + \frac{e^2}{2\pi^2} \int \frac{d^3k}{k^2} \left[ I_{++}^{(1)}(\mathbf{p}_1, \mathbf{p}_1 - \mathbf{k}) I_{++}^{(2)}(\mathbf{p}_2, \mathbf{p}_2 + \mathbf{k}) - \mathcal{B}' \right] \Psi_{++}(\mathbf{p}_1 - \mathbf{k}, \mathbf{p}_2 + \mathbf{k})
\end{aligned} \tag{A.6}$$

where

$$\mathcal{B}' = \alpha_{++}^{(1)}(\mathbf{p}_1, \mathbf{p}_1 - \mathbf{k}) \cdot \alpha_{++}^{(2)}(\mathbf{p}_2, \mathbf{p}_2 - \mathbf{k}) - \frac{\alpha_{++}^{(1)} \cdot \mathbf{k} (\alpha_{++}^{(2)} \cdot \mathbf{k})}{k^2} \tag{A.7}$$

and where

$$E(p) = +\sqrt{(mc^2)^2 + (pc)^2} \tag{A.8}$$

and where  $I_{++}^{(1)}$  and  $\alpha_{++}^{(1)}$  are represented as per the Dirac definitions

$$I_{++}(\mathbf{p}_1, \mathbf{p}_2) = \left\{ 1 + \frac{c^2(\boldsymbol{\sigma} \cdot \mathbf{p}_1)(\boldsymbol{\sigma} \cdot \mathbf{k}) + (\mathbf{E}_1 - \mathbf{E}_0)(\mathbf{E}_1 - \mathbf{E}_2)}{2E_1(E_0 + E_2)} \right\} \tag{A.9}$$

$$\alpha_{++}(\mathbf{p}_1, \mathbf{p}_2) = \frac{c}{2E_1} \left\{ \mathbf{p}_1 - i\mathbf{p}_1 \times \boldsymbol{\sigma} + \frac{E_0 + E_1}{E_0 + E_2} (\mathbf{p}_2 + i\mathbf{p}_2 \times \boldsymbol{\sigma}) \right\} \tag{A.10}$$

such that all reference to negative energy states has been removed. This equation can be expanded in powers of  $p/mc$  and  $k/mc$  up to order  $\alpha^2$ , in addition to expanding the integrand in Eq.A.6 in the same powers such that we keep only terms up to  $1/c^2$ .

Rewriting  $I_{++}$ , the Pauli approximation for this system is

$$\begin{aligned}
& \left[ W - \frac{1}{2m}(p_1^2 + p_2^2) + \frac{1}{8m^3c^2}(p_1^4 + p_2^4) \right] \Psi(\mathbf{p}_1, \mathbf{p}_2) = \\
& - e \int d^3k \phi(-\mathbf{k}) \left\{ \left[ 1 + \frac{\mathbf{p}_1 \cdot \mathbf{k} + i\sigma_1 \cdot (\mathbf{p}_1 \times \mathbf{k})}{(2mc)^2} \right] \Psi(\mathbf{p}_1 + \mathbf{k}, \mathbf{p}_2) \right. \\
& + \left. \left[ 1 + \frac{\mathbf{p}_2 \cdot \mathbf{k} + i\sigma_2 \cdot (\mathbf{p}_2 \times \mathbf{k})}{(2mc)^2} \right] \Psi(\mathbf{p}_1, \mathbf{p}_2 + \mathbf{k}) \right\} + \frac{e^2}{2\pi^2} \int \frac{d^3k}{k^2} \left\{ 1 \right. \\
& + \left. \frac{(\mathbf{p}_2 - \mathbf{p}_1) \cdot \mathbf{k} - i\sigma_1 \cdot (\mathbf{p}_1 \times \mathbf{k}) + i\sigma_2 \cdot (\mathbf{p}_2 \times \mathbf{k})}{(2mc)^2} \right\} \Psi(\mathbf{p}_1 - \mathbf{k}, \mathbf{p}_2 + \mathbf{k}) \\
& - \frac{e^2}{2\pi^2(2mc)^2} \int \frac{d^3k}{k^2} \left\{ 4 \left[ \mathbf{p}_1 \cdot \mathbf{p}_2 - \frac{(\mathbf{p}_1 \cdot \mathbf{k})(\mathbf{p}_2 \cdot \mathbf{k})}{k^2} \right] \right. \\
& + 2i [\sigma_2 \cdot (\mathbf{p}_1 \times \mathbf{k}) - \sigma_1 \cdot (\mathbf{p}_2 \times \mathbf{k})] \\
& + \left. [k^2 \sigma_1 \cdot \sigma_2 - (\sigma_1 \cdot \mathbf{k})(\sigma_2 \cdot \mathbf{k})] \right\} \Psi(\mathbf{p}_1 - \mathbf{k}, \mathbf{p}_2 + \mathbf{k}) \\
& + \frac{e}{2mc} \int d^3k \mathbf{A}(-\mathbf{k}) \cdot \{ (2\mathbf{p}_1 + i\mathbf{k} \times \sigma_1) \Psi(\mathbf{p}_1 + \mathbf{k}, \mathbf{p}_2) \\
& + (2\mathbf{p}_2 + i\mathbf{k} \times \sigma_2) \Psi(\mathbf{p}_1, \mathbf{p}_2 + \mathbf{k}) \}
\end{aligned} \tag{A.11}$$

where the first term in parentheses represents the interaction with the external electric field, the second term represents the Coulomb interaction between the two electrons, the third term represents the interaction between the electrons and the quantized radiation field, and the fourth term represents the interaction with the external magnetic field [24].

While working in momentum space is convenient for determining these representations, it is more practically convenient to work in position space, and so now another Fourier transform is performed to return to position space. We arrive at the results

quoted in Section 3, with each of the contributing Hamiltonians displayed as

$$\begin{aligned}
H_0 &= -eV + \frac{1}{2m}(p_1^2 + p_2^2) \\
H_1 &= -\frac{1}{8m^3c^2}(p_1^4 + p_2^4) \\
H_2 &= -\frac{e^2}{2(mc)^2} \frac{1}{r_{12}} \left[ \mathbf{p}_1 \cdot \mathbf{p}_2 + \frac{\mathbf{r}_{12} \cdot (\mathbf{r}_{12} \cdot \mathbf{p}_1) \mathbf{p}_2}{r_{12}^2} \right] \\
H_3 &= \frac{\mu}{mc} \left\{ \left[ \boldsymbol{\xi}_1 \times \mathbf{p}_1 + \frac{2e}{r_{12}^3} \mathbf{r}_{12} \times \mathbf{p}_2 \right] \cdot \mathbf{s}_1 + \left[ \boldsymbol{\xi}_2 \times \mathbf{p}_2 + \frac{2e}{r_{12}^3} \mathbf{r}_{21} \times \mathbf{p}_1 \right] \cdot \mathbf{s}_2 \right\} \\
H_4 &= \frac{ie\hbar}{(2mc)^2} (\mathbf{p}_1 \cdot \boldsymbol{\xi}_1 + \mathbf{p}_2 \cdot \boldsymbol{\xi}_2) \\
H_5 &= 4\mu^2 \left\{ -\frac{8\pi}{3} (\mathbf{s}_1 \cdot \mathbf{s}_2) \delta^{(3)}(\mathbf{r}_{12}) + \frac{1}{r_{12}^3} \left[ \mathbf{s}_1 \cdot \mathbf{s}_2 - \frac{3(\mathbf{s}_1 \cdot \mathbf{r}_{12})(\mathbf{s}_2 \cdot \mathbf{r}_{12})}{r_{12}^2} \right] \right\} \\
H_6 &= 2\mu [\mathcal{H}_1 \cdot \mathbf{s}_1 + \mathcal{H}_2 \cdot \mathbf{s}_2] + \frac{e}{mc} [\mathbf{A}_1 \cdot \mathbf{p}_1 + \mathbf{A}_2 \cdot \mathbf{p}_2]
\end{aligned}$$

where

$$V = \frac{Ze}{r_1} + \frac{Ze}{r_2} - \frac{e}{r_{12}} + \varphi(r_1) + \varphi(r_2), \quad \mu = \frac{e\hbar}{2mc} \quad (\text{A.12})$$

where  $V$  in  $H_0$ ,  $H_4$ , and the  $\xi$  portions of  $H_3$  correspond to the first two curly brackets in Eq. A.11. Note here that  $\boldsymbol{\xi}_1 = -\nabla_1 V$  is the Coulomb field originating from the nucleus in addition to the second electron and any external field. Further, the  $H_2$  term, the  $r_{12}$  parts of  $H_3$ , and  $H_5$  correspond to the entirety of the third curly bracket in Eq.A.11, and the final curly bracket corresponds, as expected, to the  $H_6$  term. Here we have found the path from Dirac one-electron theory to the goal of the Breit equation for a two-electron system.

# Appendix B

## Computational Details

In this section we take a closer look at the relativistic corrections, of order  $\alpha^2$ , as described in Eq.4.1. The focus is on the expression inside of the square brackets, the perturbation of each state by each contributing Hamiltonian from the Breit interaction. Start by isolating the focus of the calculation, and rewriting it as

$$\begin{aligned} T &= T_1 + T_2 \\ T &= \sum_n^N \frac{\langle \psi_{1s} | H_1 + \dots | \psi_{ns} \rangle \langle \psi_{ns} | z | \psi_{2p} \rangle}{E_{1s} - E_{ns}} + \sum_{n'}^N \frac{\langle \psi_{1s} | z | \psi_{n'p} \rangle \langle \psi_{n'p} | H_1 + \dots | \psi_{2p} \rangle}{E_{2p} - E_{n'p}} \end{aligned} \tag{B.1}$$

where the Breit interaction  $B$  is replaced by the sum of Hamiltonians. Given the essentially identical structure of  $T_1$  and  $T_2$ , we will concern ourselves only with  $T_1$ , and with the first two terms in the Breit interaction to show how the addition of multiple Hamiltonians affect the calculations. Start by defining the wave functions

$$\begin{aligned} \psi(1s) &= \sum_i^N a_i^{(1)} \chi_i^S \\ \psi(2p) &= \sum_j^N b_j^{(1)} \chi_j^P. \end{aligned} \tag{B.2}$$



where the  $a$  and  $b$  terms represent the coefficients and  $\chi$  is the wave function. This provides a basis for which to generally apply to the pseudostate form. Expressing these wave functions in their new forms yields

$$T_1 = \sum_n^N \sum_{i,i',i'',j}^N \left( \frac{a_i^{(1)} a_{i'}^{(n)} \langle \chi_i^S | H_1 | \chi_{i'}^S \rangle a_{i''}^{(n)} \langle \chi_{i''}^S | z | \chi_j^P \rangle b_j^{(1)}}{E_{1s} - E_{ns}} + \frac{a_i^{(1)} a_{i'}^{(n)} \langle \chi_i^S | H_2 | \chi_{i'}^S \rangle a_{i''}^{(n)} \langle \chi_{i''}^S | z | \chi_j^P \rangle b_j^{(1)}}{E_{1s} - E_{ns}} \right) \quad (\text{B.3})$$

such that the individual size of the basis sets for both the initial S states and the final P states is left general. Define

$$\begin{aligned} t_{i'} &= \sum_i a_i^{(1)} \langle \chi_i^S | H_1 | \chi_{i'}^S \rangle \\ z_{i''} &= \sum_j \langle \chi_{i''}^S | z | \chi_j^P \rangle b_j^{(1)} \\ d_{i'} &= \sum_i a_i^{(1)} \langle \chi_i^S | H_2 | \chi_{i'}^S \rangle \end{aligned} \quad (\text{B.4})$$

so that we can gather the summations into their own expressions. Making this change yields

$$T_1 = \sum_n^N \sum_{i',i''}^N \left( \frac{t_{i'} a_{i'}^{(n)} a_{i''}^{(n)} z_{i''}^{(n)}}{E_{1s} - E_{ns}} + \frac{d_{i'} a_{i'}^{(n)} a_{i''}^{(n)} z_{i''}^{(n)}}{E_{1s} - E_{ns}} \right) \quad (\text{B.5})$$

as the equation begins to simplify, it is important to note what the purpose is. Having the overall expression  $T_1$  in this form prescribes a calculation of the matrix elements, and a pairing with the relevant coefficients. Then define

$$\begin{aligned} u_n &= \sum_{i'}^N t_{i'} a_{i'}^{(n)} \\ v_n &= \sum_{i''}^N a_{i''}^{(n)} z_{i''}^{(n)} \\ w_n &= \sum_{i'}^N d_{i'} a_{i'}^{(n)} \end{aligned} \quad (\text{B.6})$$

to link the pseudostates with the matrix elements for each relativistic contribution, as well as the transition operator. This is now a working expression that can be calculated. The action to be taken now is to calculate the matrix elements from each contributing Hamiltonian, generate the relevant pseudostates, and then multiply these “arrays” together to form  $u_n$ ,  $v_n$  and  $w_n$ . Next, we can substitute these definitions into our main expression to find

$$T_1 = \sum_n^N \left( \frac{u_n v_n}{E_{1s} - E_{ns}} + \frac{w_n v_n}{E_{1s} - E_{ns}} \right) \quad (\text{B.7})$$

which presents the calculation in its simplest form, except for the purposeful separation of the two, in this example, contributing Hamiltonians. Adding in  $T_2$ , and finally simplifying yields

$$T = T_1 + T_2$$

$$T = \sum_n^N \frac{(u_n + w_n)v_n}{E_{1s} - E_{ns}} + \sum_{n'}^{N'} \frac{v'_{n'}(u'_n + w'_n)}{E_{2p} - E_{n'p}} \quad (\text{B.8})$$

where it can be seen that the addition of the remaining contributing Hamiltonians is as simple as adding another term inside of the parentheses. A sample of the Fortran code written for this purpose is given in Figure B below.

Listing B.1: Fortran sample of matrix multiplication

```

C      INITIAL STATE
C      P4 AND Z
      DO 135 J=1,NVI
      DO 134 I=1,NVI
      UNI(J)=UNI(J)+TRBI(I)*TOTISH(I,J)
      VNI(J)=VNI(J)+TOTISH(I,J)*TRBOI(I)
134 CONTINUE

```

```

135 CONTINUE
C      DELTA
      DO 123 K=1,5
      DO 121 J=1,NVI
      DO 122 I=1,NVI
      WNI(K, J)=WNI(K, J)+TRBDI(K, I)*TOTISH(I, J)
122 CONTINUE
121 CONTINUE
123 CONTINUE

      DO 158 I=2,NVI
      TEESP(1, I)=UNI(I)*VNI(I)/(PSI2I(1)-PSI2I(I))
      TEESD(1, I)=(WNI(1, I)+WNI(2, I)+WNI(3, I)+WNI(4, I)
1 +WNI(5, I))*VNI(I)/(PSI2I(1)-PSI2I(I))
C      SEPARATE DELTA I
      DO 162 J=1,5
      TWDI(J)=TWDI(J)+WNI(J, I)*VNI(I)/(PSI2I(1)-PSI2I(I))
162 CONTINUE
      TEES(1, I)=(UNI(I)+WNI(1, I)+WNI(2, I)+WNI(3, I)+WNI(4, I)
1 +WNI(5, I))*VNI(I)/(PSI2I(1)-PSI2I(I))
      TEE(1)=TEE(1) + TEES(1, I)
      TEEP(1)=TEEP(1) + TEESP(1, I)
      TEED(1)=TEED(1) + TEESD(1, I)
158 CONTINUE

```

# Bibliography

- [1] G. W. F. Drake, *Springer handbook of atomic, molecular, and optical physics* (Springer Science & Business Media, 2006).
- [2] G. W. F. Drake, *Phys. Rev. A* **19**, 1387 (1979).
- [3] J. Fox, in *Springer Handbook of Atomic, Molecular, and Optical Physics* (Springer, 2006) pp. 1259–1292.
- [4] E. A. Hylleraas, *Z. Phys.* **54**, 347 (1929).
- [5] D. R. Hartree, *Mathematical Proceedings of the Cambridge Philosophical Society* **24**, 89110 (1928).
- [6] G. W. F. Drake, *Phys. Rev. A* **18**, 820 (1978).
- [7] Z.-C. Yan, M. Tambasco, and G. W. F. Drake, *Phys. Rev. A* **57**, 1652 (1998).
- [8] G. W. F. Drake, *Canadian Journal of Physics* **50**, 1896 (1972).
- [9] K. T. Chung and B. F. Davis, *Phys. Rev. A* **31**, 1187 (1985).
- [10] G. W. F. Drake and Z.-C. Yan, *Phys. Rev. A* **46**, 2378 (1992).
- [11] A. Kono and S. Hattori, *Phys. Rev. A* **29**, 2981 (1984).
- [12] S. A. Alexander, S. Datta, and R. L. Coldwell, *Phys. Rev. A* **81**, 032519 (2010).
- [13] D. L. Lin, *Phys. Rev. A* **15**, 2324 (1977).

- [14] G. W. F. Drake, *Phys. Rev. A* **5**, 1979 (1972).
- [15] E. Mazur, C. H. Crouch, D. Pedigo, P. A. Dourmashkin, and R. J. Bieniek, *Principles & practice of physics* (Pearson, 2015) Chap. 13.
- [16] E. Mazur, C. H. Crouch, D. Pedigo, P. A. Dourmashkin, and R. J. Bieniek, *Principles & practice of physics* (Pearson, 2015) Chap. 25.
- [17] L. Kirkby, *Physics: A Student Companion* (Scion, 2011) Chap. 16.
- [18] J. K. L. MacDonald, *Phys. Rev. A* **43**, 830 (1933).
- [19] D. L. Actomick, (1987).
- [20] G. W. F. Drake, “Variational methods a,” in *Digital Encyclopedia of Applied Physics* (2003).
- [21] H. Bethe and E. Salpeter, *Quantum Mechanics of One- and Two-Electron Atoms* (Springer US, 2012).
- [22] M. Sami, *Nonrelativistic Operators for Relativistic Corrections to Radiative Transitions*, Master’s thesis, University of Windsor (2018).
- [23] M. Cohen and A. Dalgarno, *Proc. R. Soc. Lond. A* **280**, 258 (1964).
- [24] H. Bethe and E. Salpeter, *Quantum Mechanics of One- and Two-Electron Atoms* (Springer US, 2012) Chap. 16.

# Vita Auctoris

NAME: Daniel Venn  
PLACE OF BIRTH: Brampton, ON  
YEAR OF BIRTH: 1994  
EDUCATION: St. Anne's High School, Lakeshore, ON, 2012  
University of Windsor, B.Sc., Windsor, ON, 2016